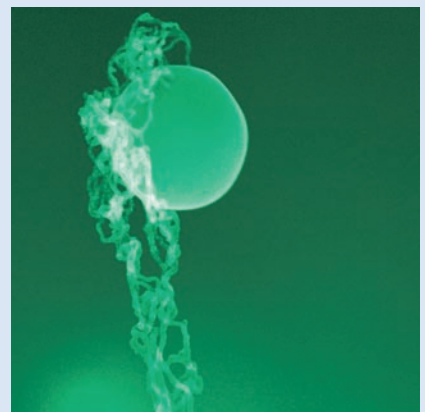
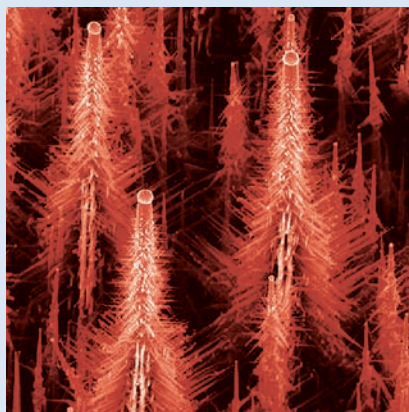
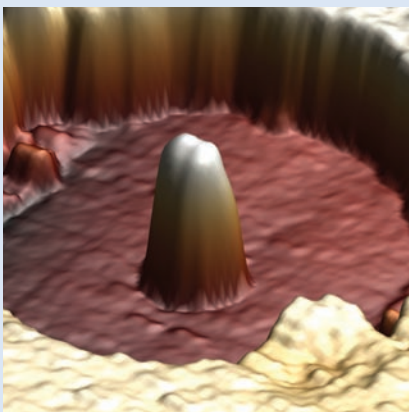
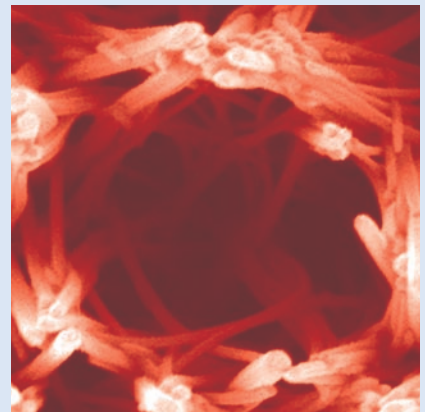
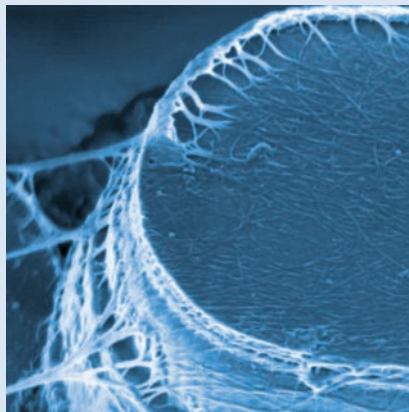
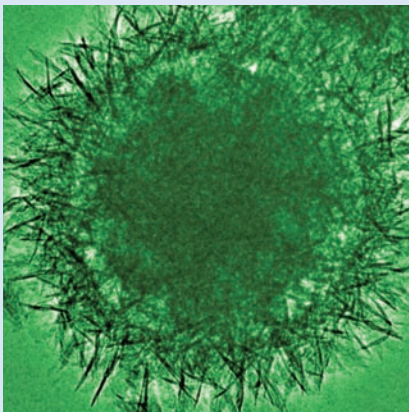
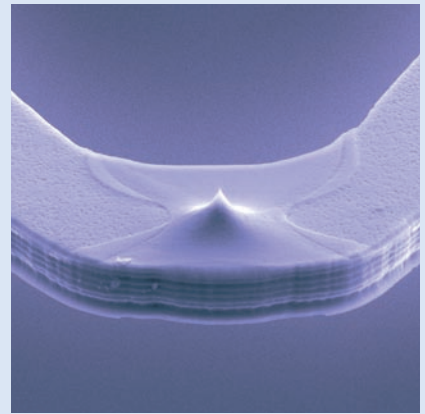
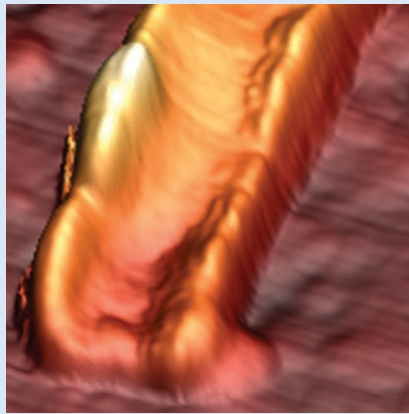
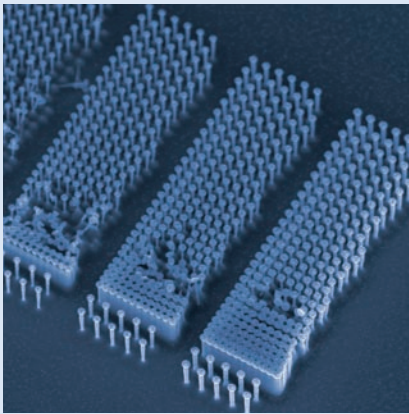


NANOTECHNOLOGY

Highlights 2009

www.iop.org/EJ/nano

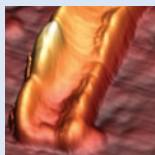


IOP Publishing

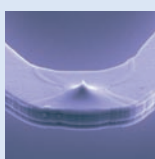
COVER IMAGES



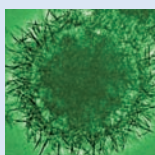
84 nm wide and 600 nm tall pillars in a matrix of variable density with a minimum pitch of 200 nm taken from the article 'The fabrication of silicon nanostructures by local gallium implantation and cryogenic deep reactive ion etching' by **N Chekurov, K Grigoras, A Peltonen, S Franssila and I Tittonen** 2009 *Nanotechnology* **20** 065307



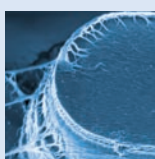
AFM image of a micrometer-long AlN nanotube taken from the article 'Elastic moduli of faceted aluminum nitride nanotubes measured by contact resonance atomic force microscopy' by **G Stan, C V Ciobanu, T P Thayer, G T Wang, J R Creighton, K P Purushotham, LA Bendersky and R F Cook** 2009 *Nanotechnology* **20** 035706



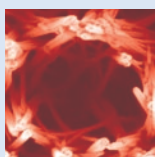
SEM image of a released nanoheater cantilever with a sharp tip taken from the article 'A 100 nanometer scale resistive heater–thermometer on a silicon cantilever' by **Z Dai, W P King and K Park** 2009 *Nanotechnology* **20** 095301



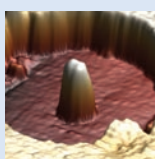
TEM image of a hierarchical SiO₂@γ-AIOOH core shell structure obtained at 160 °C for 12 hours taken from the article 'Template-induced synthesis of hierarchical SiO₂@γ-AIOOH spheres and their application in Cr(VI) removal' by **Yongqiang Wang, Guozhong Wang, Hongqiang Wang, Weiping Cai, Changhao Liang and Lide Zhang** 2009 *Nanotechnology* **20** 155604



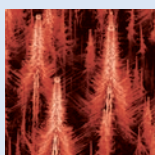
SEM micrograph of SWNTs assembled between the M2 and M3 layers of the CMOS chip taken from the article 'The heterogeneous integration of single-walled carbon nanotubes onto complementary metal oxide semiconductor circuitry for sensing applications' by **Chia-Ling Chen, Vinay Agarwal, Sameer Sonkusale and Mehmet R Dokmeci** 2009 *Nanotechnology* **20** 225302



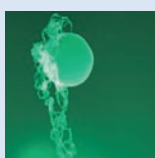
Field-emission scanning electron microscopy image of aggregated ZnO nanowires that form nanoscale structures with superhydrophobic properties taken from the article 'A reticulate superhydrophobic self-assembly structure prepared by ZnO nanowires' by **Maogang Gong, Xiaoliang Xu, Zhou Yang, Yuanyue Liu, Haifei Lv and Liu Lv** 2009 *Nanotechnology* **20** 165602



The eruption of oxygen gas produced by electro-reduction in a metal/oxide/metal multilayer thin film junction leaves a crater 40 nm deep and about 600 nm wide, with a pillar 150 nm in diameter and 40 nm tall at the centre taken from the article 'The mechanism of electroforming of metal oxide memristive switches' by **J Joshua Yang, Feng Miao, Matthew D Pickett, Douglas A A Ohlberg, Duncan R Stewart, Chun Ning Lau and R Stanley Williams** 2009 *Nanotechnology* **20** 215201

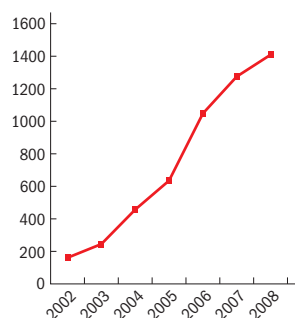


SEM image showing a tilted view of nanotrees grown at 650 °C taken from the article 'The morphology of silicon nanowires grown in the presence of trimethylaluminium' by **F Oehler, P Gentile, T Baron, M Den Hertog, J Rouvière and P Ferret** 2009 *Nanotechnology* **20** 245602

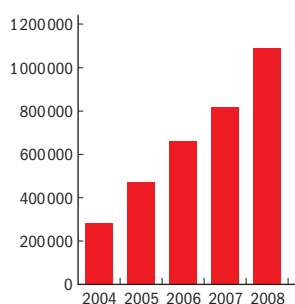


Close-up of droplet and silicon oxide nanowire consisting of several precipitated oxide strands taken from the article 'Low-temperature vapour–liquid–solid (VLS) growth of vertically aligned silicon oxide nanowires using concurrent ion bombardment' by **Martin Bettge, Scott MacLaren, Steve Burdin, Jian-Guo Wen, Daniel Abraham, Ivan Petrov and Ernie Sammann** 2009 *Nanotechnology* **20** 115607

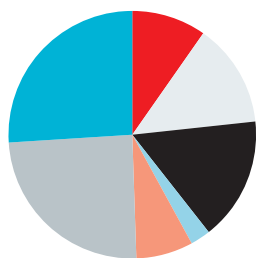
Articles published



Yearly downloads



Subject distribution



- Biology and medicine
- Electronics and photonics
- Patterning and nanofabrication
- Quantum phenomena
- Sensing and actuating
- Materials: synthesis or self assembly
- Materials: properties, characterization or tools

Dear Colleague,

Looking back over the past 12 months, 2009 has been a particularly favourable year for *Nanotechnology*. The journal has celebrated its 20th volume, an exciting landmark for what was the first ever academic publication in its field.

Since the journal was launched in 1990, research in nanotechnology has experienced an explosive boom, and this has also been reflected in the growth of the journal *Nanotechnology*. In recent years the number of articles published has soared as the journal has moved from a monthly to a weekly publication; *Nanotechnology* now publishes nearly five times as many articles a year as many of its leading competitors.

At the same time the journal excels in terms of speed of publication; the time taken for a first decision to be made on each article submitted is now 21 days. Articles hot off the press at *Nanotechnology* truly do represent the very latest and most topical research in the field.

Accompanying the growth in total content, an increase in the quality of the articles published has also been sustained, as reflected in this year's ISI impact factor. The excellent quality of the journal's content is what this compendium of highlights from 2009 is designed to celebrate. Among the articles in this collection is an atomic force microscope study where high-resolution topographical images of carbon nanotubes on the nuclear membrane in cells are presented. The work demonstrates the potential of atomic force microscopy for monitoring the transport of individual carbon nanotubes through single nuclear pore complexes into the cell nucleus. In another article Yaping Dan and colleagues from the USA and Canada report a conducting polymer nanowire sensor that can detect a variety of substances at concentrations of parts per million with high device-to-device reproducibility. The results constitute a significant advance towards the development of a low-footprint, versatile 'electronic nose'.

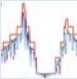

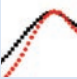


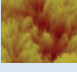
This collection of highlights from 2009 reflects the breadth of the journal's scope and includes articles on biology and medicine, electronics and photonics, patterning and fabrication, sensing and actuating, quantum phenomena and the synthesis and properties of nanomaterials. The articles are a taster of recent developments in science at the nanoscale, and indicate an inspiring level of research activity with much to look forward to in *Nanotechnology*.

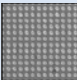
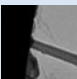
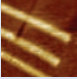
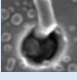
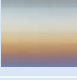
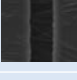

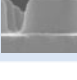


Professor Mark Reed
 Editor-in-Chief, *Nanotechnology*
 E-mail: nano@iop.org
www.iop.org/EJ/nano

CONTENTS

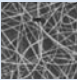
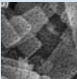

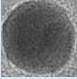

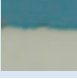
BIOLOGY AND MEDICINE		PAGE
	Mn-doped near-infrared quantum dots as multimodal targeted probes for pancreatic cancer imaging Ken-Tye Yong	8
	Carbon nanotube self-assembly with lipids and detergent: a molecular dynamics study E Jayne Wallace and Mark S P Sansom	8
	Bio-conjugated luminescent quantum dots of doped ZnS: a cyto-friendly system for targeted cancer imaging Koyakutty Manzoor, Seby Johny, Deepa Thomas, Sonali Setua, Deepthy Menon and Shantikumar Nair	8
	Aqueous synthesis of type-II CdTe/CdSe core-shell quantum dots for fluorescent probe labeling tumor cells Ruosheng Zeng, Tingting Zhang, Jincheng Liu, Song Hu, Qiang Wan, Xuanming Liu, Zhiwei Peng and Bingsuo Zou	9
	Nanosized zinc oxide particles induce neural stem cell apoptosis Xiaoyong Deng, Qixia Luan, Wenting Chen, Yanli Wang, Minghong Wu, Haijiao Zhang and Zheng Jiao	9
	Magnetic chitosan nanoparticles as a drug delivery system for targeting photodynamic therapy Yun Sun, Zhi-long Chen, Xiao-xia Yang, Peng Huang, Xin-ping Zhou and Xiao-xia Du	10
	Simultaneous mechanical stiffness and electrical potential measurements of living vascular endothelial cells using combined atomic force and epifluorescence microscopy Chiara Callies, Peter Schön, Ivan Liashkovich, Christian Stock, Kristina Kusche-Vihrog, Johannes Fels, Alexandra S Sträter and Hans Oberleithner	10
	Biologically inspired rosette nanotubes and nanocrystalline hydroxyapatite hydrogel nanocomposites as improved bone substitutes Lijie Zhang, Jose Rodriguez, Jose Raez, Andrew J Myles, Hicham Fenniri and Thomas J Webster	10
	Reverse DNA translocation through a solid-state nanopore by magnetic tweezers Hongbo Peng and Xinsheng Sean Ling	11
	AFM imaging of functionalized carbon nanotubes on biological membranes C Lamprecht, I Liashkovich, V Neves, J Danzberger, E Heister, M Rangl, H M Coley, J McFadden, E Flahaut, H J Gruber, P Hinterdorfer, F Kienberger and A Ebner	11

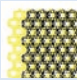
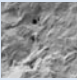
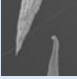




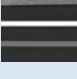
ELECTRONICS AND PHOTONICS		PAGE
	The effects of defects on the conductance of graphene nanoribbons Narjes Gorjizadeh, Amir A Farajian and Yoshiyuki Kawazoe	12
	Resistive switching characteristics of polymer non-volatile memory devices in a scalable via-hole structure Tae-Wook Kim, Hyejung Choi, Seung-Hwan Oh, Minseok Jo, Gunuk Wang, Byungjin Cho, Dong-Yu Kim, Hyunsang Hwang and Takhee Lee	12
	Ordered polythiophene/fullerene composite core-shell nanorod arrays for solar cell applications Hsu-Shen Wang, Li-Hua Lin, Shih-Yung Chen, Yuh-Lin Wang and Kung-Hwa Wei	12
	Flexible photovoltaic cells fabricated utilizing ZnO quantum dot/carbon nanotube heterojunctions Fushan Li, Dong Ick Son, Sung Hwan Cho, Won Tae Kim and Tae Whan Kim	13
	Electrical properties of individual ZnO nanowires M Sakurai, Y G Wang, T Uemura and M Aono	13
	High efficiency polymer solar cells with vertically modulated nanoscale morphology Ankit Kumar, Gang Li, Ziruo Hong and Yang Yang	14

PATTERNING AND NANOFABRICATION		PAGE
	Surface-plasmon-enhanced fluorescence from periodic quantum dot arrays through distance control using biomolecular linkers Melvin T Zin, Kirsty Leong, Ngo-Yin Wong, Hong Ma, Mehmet Sarikaya and Alex K-Y Jen	14
	Nanoslits in silicon chips Thomas Aref, Matthew Brenner and Alexey Bezyradin	14
	Real-time nanofabrication with high-speed atomic force microscopy J A Vicary and M J Miles	15
	Guiding vapor-liquid-solid nanowire growth using SiO₂ Nathaniel J Quitarano, Wei Wu and Theodore I Kamins	15
	Nanofluidic structures with complex three-dimensional surfaces Samuel M Stavis, Elizabeth A Strychalski and Michael Gaitan	15
	The fabrication of ZnO nanowire field-effect transistors by roll-transfer printing Yi-Kuei Chang and Franklin Chau-Nan Hong	16
	Nanolithography based on an atom pinhole camera P N Melentiev, A V Zablotskiy, D A Lapshin, E P Sheshin, A S Baturin and V I Balykin	16
	Nanopost plasmonic crystals T T Truong, J Maria, J Yao, M E Stewart, T-W Lee, S K Gray, R G Nuzzo and J A Rogers	16

Continues...

QUANTUM PHENOMENA		PAGE
	An InGaN/GaN single quantum well improved by surface modification of GaN films Z L Fang, J Y Kang and W Z Shen	17
	Interface states and bio-conjugation of CdSe/ZnS core-shell quantum dots T V Torchynska	17
	A fully coherent electron beam from a noble-metal covered W(111) single-atom emitter Che-Cheng Chang, Hong-Shi Kuo, Ing-Shouh Hwang and Tien T Tsong	17
	Thermoelectromechanical effects in quantum dots Sunil R Patil and Roderick V N Melnik	18
	Thermal conductivity of carbon nanotubes with quantum correction via heat capacity Michael C H Wu and Jang-Yu Hsu	18
	Atomic layer deposition of quantum-confined ZnO nanostructures David M King, Samantha I Johnson, Jianhua Li, Xiaohua Du, Xinhua Liang and Alan W Weimer	18
MATERIALS: SYNTHESIS OR SELF-ASSEMBLY		PAGE
	Hierarchically organized nanostructured TiO₂ for photocatalysis applications F Di Fonzo, C S Casari, V Russo, M F Brunella, A Li Bassi and C E Bottani	19
	Self-aligned growth of single-walled carbon nanotubes using optical near-field effects W Xiong, Y S Zhou, M Mahjouri-Samani, W Q Yang, K J Yi, X N He, S H Liou and Y F Lu	19
	Photo-induced effects on self-organized TiO₂ nanotube arrays: the influence of surface morphology A G Kontos, A I Kontos, D S Tsoukleris, V Likodimos, J Kunze, P Schmuki and P Falaras	20
	Three-dimensional electrodes for dye-sensitized solar cells: synthesis of indium-tin-oxide nanowire arrays and ITO/TiO₂ core-shell nanowire arrays by electrophoretic deposition Hong-Wen Wang, Chi-Feng Ting, Miao-Ken Hung, Chwei-Huann Chiou, Ying-Ling Liu, Zongwen Liu, Kyle R Ratinac and Simon P Ringer	20
	Spray deposition of steam treated and functionalized single-walled and multi-walled carbon nanotube films for supercapacitor Xin Zhao, Bryan T T Chu, Belén Ballesteros, Weiliang Wang, Colin Johnston, John M Sykes and Patrick S Grant	21
	Graphene on insulating crystalline substrates S Akcöltekin, M El Kharrazi, B Köhler, A Lorke and M Schleberger	21
	A novel method for metal oxide nanowire synthesis Simas Rackauskas, Albert G Nasibulin, Hua Jiang, Ying Tian, Victor I Kleshch, Jani Sainio, Elena D Obratsova, Sofia N Bokova, Alexander N Obratsov and Esko I Kauppinen	21
	Templated growth of graphenic materials Nolan W Nicholas, L Matthew Connors, Feng Ding, Boris I Yakobson, Howard K Schmidt and Robert H Hauge	22
	Ultrafast VLS growth of epitaxial β-Ga₂O₃ nanowires E Auer, A Lugstein, S Löffler, Y J Hyun, W Brezna, E Bertagnolli and P Pongratz	22

SENSING AND ACTUATING		PAGE
	A highly sensitive ethanol sensor based on mesoporous ZnO–SnO₂ nanofibers Xiaofeng Song, Zhaojie Wang, Yongben Liu, Ce Wang and Lijuan Li	22
	Novel porous single-crystalline ZnO nanosheets fabricated by annealing ZnS(en)_{0.5} (en = ethylenediamine) precursor. Application in a gas sensor for indoor air contaminant detection Jinyun Liu, Zheng Guo, Fanli Meng, Tao Luo, Minqiang Li and Jinhuai Liu	23
	Carbon nanotube-based ethanol sensors Sean Brahim, Steve Colbern, Robert Gump, Alex Moser and Leonid Grigorian	23
	Non-functionalized silver nanoparticles for a localized surface plasmon resonance-based glucose sensor A Serra, E Filippo, M Re, M Palmisano, M Vittori-Antisari, A Buccolieri and D Manno	23
	A new multifunctional platform based on high aspect ratio interdigitated NEMS structures S Ghatnekar-Nilsson, I Karlsson, A Kvennefors, G Luo, V Zela, M Arlelid, T Parker, L Montelius and A Litwin	24
	Gas sensing properties of single conducting polymer nanowires and the effect of temperature Yaping Dan, Yanyan Cao, Tom E Mallouk, Stephane Evoy and A T Charlie Johnson	24

MATERIALS: PROPERTIES CHARACTERIZATION AND TOOLS		PAGE
	Effective elastic mechanical properties of single layer graphene sheets F Scarpa, S Adhikari and A Srikantha Phani	24
	The mechanical properties and morphology of a graphite oxide nanosheet/polyurethane composite Dongyu Cai, Kamal Yusoh and Mo Song	25
	Fabrication and characterization of a carbon nanotube-based nanoknife G Singh, P Rice, R L Mahajan and J R McIntosh	25
	Fabrication and photocatalytic activities in visible and UV light regions of Ag@TiO₂ and NiAg@TiO₂ nanoparticles Haw-Yeu Chuang and Dong-Hwang Chen	26
	Nano-indentation studies on polymer matrix composites reinforced by few-layer grapheme Barun Das, K Eswar Prasad, U Ramamurty and C N R Rao	26
	Fabrication of porous carbon nanofibers and their application as anode materials for rechargeable lithium-ion batteries Liwen Ji and Xiangwu Zhang	27
	A new AFM–HRTEM combined technique for probing isolated carbon nanotubes Shota Kuwahara, Toshiki Sugai and Hisanori Shinohara	27
	Measuring the surface-enhanced Raman scattering enhancement factors of hot spots formed between an individual Ag nanowire and a single Ag nanocube Pedro H C Camargo, Claire M Cobley, Matthew Rycenga and Younan Xia	27

LIST OF EDITORS		PAGE
Editorial Board and Journal Team		28

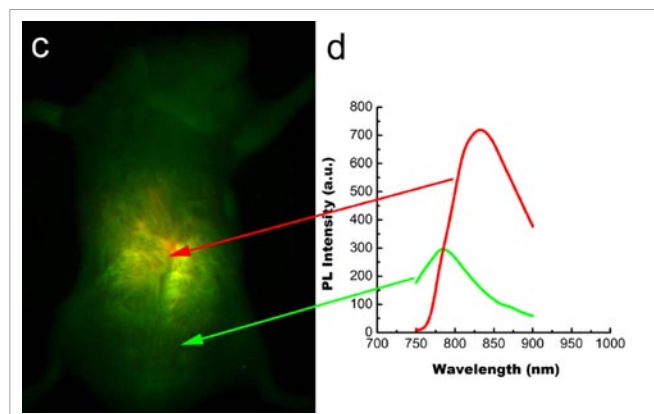
BIOLOGY AND MEDICINE

Mn-doped near-infrared quantum dots as multimodal targeted probes for pancreatic cancer imaging

Ken-Tye Yong

Institute for Lasers, Photonics and Biophotonics, University at Buffalo, State University of New York, Buffalo, NY 14260-4200, USA

This work presents a novel approach to producing manganese (Mn)-doped quantum dots (Mnd-QDs) emitting in the near-infrared (NIR). Surface functionalization of Mnd-QDs with lysine makes them stably disperse in aqueous media and able to conjugate with targeting molecules. The nanoparticles were structurally and compositionally characterized and maintained a high photoluminescence quantum yield and displayed paramagnetism in water. The receptor-mediated delivery of bioconjugated Mnd-QDs into pancreatic cancer cells was demonstrated using the confocal microscopy technique. Cytotoxicity of Mnd-QDs on live cells has been evaluated. The NIR-emitting characteristic of the QDs has been exploited to acquire whole animal body imaging with high contrast signals. In addition, histological and blood analysis of mice have revealed that no long-term toxic effects arise from Mnd-QDs. These studies suggest multimodal Mnd-QDs have the potentials as probes for early pancreatic cancer imaging and detection.



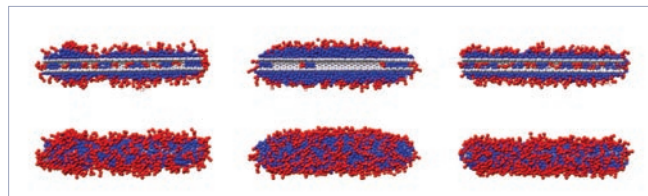
Overlay of two NIR fluorescence images from a mouse injected with Mn-doped NIR QDs (green = background autofluorescence from the mouse and red = NIR QD signal), plus the corresponding spectra of autofluorescence and QDs.

Carbon nanotube self-assembly with lipids and detergent: a molecular dynamics study

E Jayne Wallace and Mark S P Sansom

Department of Biochemistry, University of Oxford, South Parks Road, Oxford OX1 3QU, UK

The dispersion of carbon nanotubes (CNTs) in aqueous media is of potential importance in a number of biomedical applications. CNT solubilization has been achieved via the non-covalent adsorption of lipids and detergent onto the tube surface. We use coarse-grained molecular dynamics to study the self-assembly of CNTs with various amphiphiles, namely a bilayer-forming lipid, dipalmitoylphosphatidylcholine (DPPC), and two species of detergent, dihexanoylphosphatidylcholine (DHPC) and lysophosphatidylcholine (LPC). We find that for a low amphiphile/CNT ratio, DPPC, DHPC and LPC all wrap around the CNT. Upon increasing the number of amphiphiles, a transition in adsorption is observed: DPPC encapsulates the CNT within a cylindrical micelle, whilst both DHPC and LPC adsorb onto CNTs in hemimicelles. This study highlights differences in adsorption mechanism of bilayer-forming lipids and detergents on CNTs which may in the future be exploitable to enable enhancement of CNT solubilization whilst minimizing perturbation of cell membrane integrity.



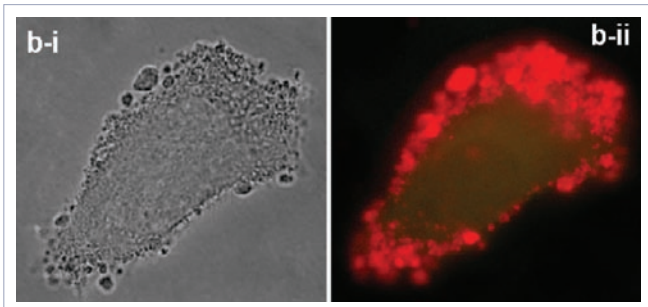
Snapshots of amphiphile self-assembly onto a CNT ((a) LPC, (b) DPPC and (c) DHPC); the hydrophilic headgroup particles are shown in red, and the hydrophobic tail particles are shown in blue.

Bio-conjugated luminescent quantum dots of doped ZnS: a cyto-friendly system for targeted cancer imaging

Koyakutty Manzoor, Seby Johny, Deepa Thomas, Sonali Setua, Deepthy Menon and Shantikumar Nair

Amrita Centre for Nanoscience, Amrita Institute of Medical Science and Research Centre, Cochin 682026, Kerala, India

A heavy-metal-free luminescent quantum dot (QD) based on doped zinc sulfide (ZnS), conjugated with a cancer-targeting ligand, folic acid (FA), is presented as a promising bio-friendly system for targeted cancer imaging. Doped QDs were prepared by a simple aqueous method at room temperature. X-ray diffraction and transmission electron microscopy studies showed the formation of monodisperse QDs of average size ~ 4 nm with cubic (sphalerite) crystal structure. Doping of the QDs with metals (Al^{3+}), transition metals (Cu^+ , Mn^{2+}) and halides (F^-) resulted in multi-color emission with dopant-specific color tunability ranging from blue (480 nm) to red (622 nm). Luminescent centers in doped QDs could be excited using bio-friendly visible light >400 nm by directly populating the dopant centers, leading to bright emission. The cytotoxicity of bare and FA conjugated QDs was tested *in vitro* using normal lung fibroblast cell line (L929), folate-receptor-positive (FR+) nasopharyngeal epidermoid carcinoma cell line (KB), and FR-negative (FR-) lung cancer cell line (A549). Both bare and FA-conjugated ZnS QDs elicited no apparent toxicity even at high concentrations of $\sim 100 \mu M$ and 48 h of incubation. In contrast, CdS QDs prepared under identical conditions showed relatively high toxicity even at low concentrations of $\sim 0.1 \mu M$ and 24 h of incubation. Interaction of FA-QDs with different cell lines showed highly specific attachment of QDs in the FR+ cancer cell line, leaving others unaffected. The bright and stable luminescence of the QDs could be used to image both single cancer cells and colonies of cancer cells without affecting their metabolic activity and morphology. Thus, this study presents, for the first time, the use of non-toxic, Cd-, Te-, Se-, Pb- and Hg-free luminescent QDs for targeted cancer imaging.



Bright-field image of carcinoma cells with QDs attached to the cell membrane and the corresponding true color fluorescence image showing a large aggregation of red-emitting QDs on the cell membrane.

Aqueous synthesis of type-II CdTe/CdSe core-shell quantum dots for fluorescent probe labeling tumor cells

Featured on
nanotechweb.org

Ruosheng Zeng^{1,2}, Tingting Zhang^{1,3}, Jincheng Liu⁴, Song Hu¹, Qiang Wan¹, Xuanming Liu⁵, Zhiwei Peng¹ and Bingsuo Zou^{4,6,7}

¹ State Key Lab of CSBC, and Micro-Nano Center, Hunan University, Changsha 410082, People's Republic of China

² Department of Chemistry and Biochemistry, University of Arkansas, Fayetteville, AR 72701, USA

³ Institute of Plant Source Utilization, Hunan Agricultural University, Changsha 410128, People's Republic of China

⁴ Institute of Polymer Optoelectronic Materials and Devices, South China University of Technology, Guangzhou 510640, People's Republic of China

⁵ Institute of Life Science and Biotechnology, Hunan University, Changsha 410082, People's Republic of China

⁶ School of Material Science and Engineering, Beijing Institute of Technology, Beijing 100081, People's Republic of China

In this paper, we report a two-step aqueous synthesis of highly luminescent CdTe/CdSe core/shell quantum dots (QDs) via a simple method. The emission range of the CdTe/CdSe QDs can be tuned from 510 to 640 nm by controlling the thickness of the CdSe shell. Accordingly, the photoluminescence quantum yield (PL QY) of CdTe/CdSe QDs with an optimized thickness of the CdSe shell can reach up to 40%. The structures and compositions of the core/shell QDs were characterized by transmission electron microscopy, x-ray diffraction, and x-ray photoelectron spectroscopy experiments, and their formation mechanism is discussed. Furthermore, folate conjugated CdTe/CdSe QDs in HeLa cells were assessed with a fluorescence microscope. The results show that folate conjugated CdTe/CdSe QDs could enter tumor cells efficiently.



Photograph of the wide spectral range of bright luminescence from the sample of CdTe core QDs (a) and CdTe/CdSe QDs ((b)-(d)) dispersed in water.

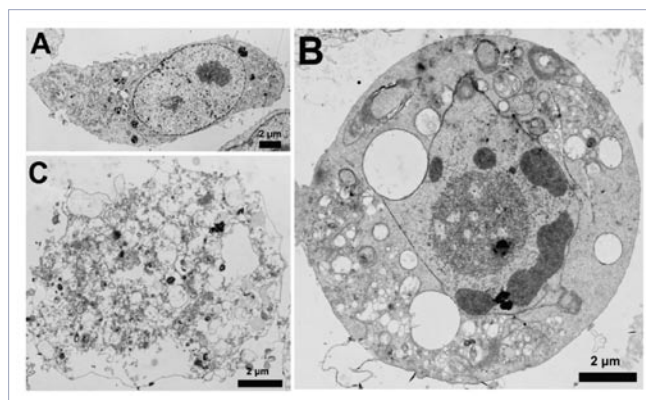
Nanosized zinc oxide particles induce neural stem cell apoptosis

Xiaoyong Deng¹, Qixia Luan¹, Wenting Chen², Yanli Wang², Minghong Wu^{1,2}, Haijiao Zhang¹ and Zheng Jiao¹

¹ Institute of Nanochemistry and Nanobiology, Shanghai University, Shanghai 200444, People's Republic of China

² School of Environmental and Chemical Engineering, Shanghai University, Shanghai 200444, People's Republic of China

Given the intensive application of nanoscale zinc oxide (ZnO) materials in our life, growing concerns have arisen about its unintentional health and environmental impacts. In this study, the neurotoxicity of different sized ZnO nanoparticles in mouse neural stem cells (NSCs) was investigated. A cell viability assay indicated that ZnO nanoparticles manifested dose-dependent, but no size-dependent toxic effects on NSCs. Apoptotic cells were observed and analyzed by confocal microscopy, transmission electron microscopy examination, and flow cytometry. All the results support the viewpoint that the ZnO nanoparticle toxicity comes from the dissolved Zn²⁺ in the culture medium or inside cells. Our results highlight the need for caution during the use and disposal of ZnO manufactured nanomaterials to prevent the unintended environmental and health impacts.



TEM images of control neural stem cells (A) and early (B) or advanced (C) apoptotic neural stem cells treated with ZnO nanoparticles.

Get the latest
Nanotechnology research
sent straight to you!

Sign up for free e-mail alerts at
www.iop.org/EJ/Nano

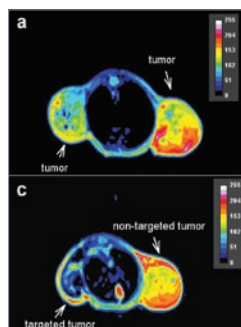
Magnetic chitosan nanoparticles as a drug delivery system for targeting photodynamic therapy

Yun Sun¹, Zhi-long Chen^{1,3}, Xiao-xia Yang¹, Peng Huang¹, Xin-ping Zhou¹ and Xiao-xia Du²

¹ Department of Pharmaceutical Science and Technology, College of Chemistry and Biology, Donghua University, Shanghai 201620, People's Republic of China

² Department of Physics, East China Normal University, Shanghai 200062, People's Republic of China

Photodynamic therapy (PDT) has become an increasingly recognized alternative to cancer treatment in clinic. However, PDT therapy agents, namely photosensitizer (PS), are limited in application as a result of prolonged cutaneous photosensitivity, poor water solubility and inadequate selectivity, which are encountered by numerous chemical therapies. Magnetic chitosan nanoparticles provide excellent biocompatibility, biodegradability, non-toxicity and water solubility without compromising their magnetic targeting. Nevertheless, no previous attempt has been reported to develop an *in vivo* magnetic drug delivery system with chitosan nanoparticles for magnetic resonance imaging (MRI) monitored targeting photodynamic therapy. In this study, magnetic targeting chitosan nanoparticles (MTCNPs) were prepared and tailored as a drug delivery system and imaging agents for PS, designated as PHPP. Results showed that PHPP-MTCNPs could be used in MRI monitored targeting PDT with excellent targeting and imaging ability. Non-toxicity and high photodynamic efficacy on SW480 carcinoma cells both *in vitro* and *in vivo* were achieved with this method at the level of 0–100 μM . Notably, localization of nanoparticles in skin and hepatic tissue was significantly less than in tumor tissue, therefore photosensitivity and hepatotoxicity can be attenuated.



Magnetic resonance images of non-targeted (top) and targeted (bottom) double grafted tumor system. No significant difference was observed between the left and right tumor in non-targeted mice, but the externally localized magnetic field at the left tumor surface resulted in the significant darkening of MR images, compared to the non-targeted tumor on the right.

Simultaneous mechanical stiffness and electrical potential measurements of living vascular endothelial cells using combined atomic force microscopy and epifluorescence microscopy

Featured on
nanotechweb.org

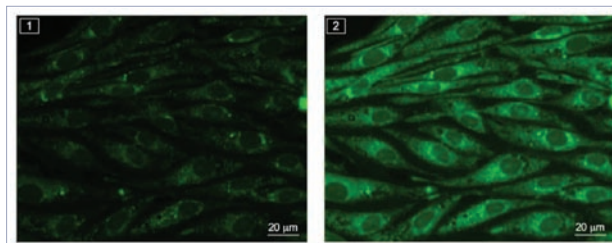
Chiara Callies^{1,3}, Peter Schön², Ivan Liashkovich¹, Christian Stock¹, Kristina Kusche-Vihrog¹, Johannes Fels¹, Alexandra S Sträter¹ and Hans Oberleithner¹

¹ Institute of Physiology II, University of Münster, Germany

² Veeco Instruments GmbH, Life Science Team, Mannheim, Germany

³ Address for correspondence: Institute of Physiology II, Robert-Koch-Strasse 27b, 48149 Münster, Germany

The degree of mechanical stiffness of vascular endothelial cells determines the endogenous production of the vasodilating gas nitric oxide (NO). However, the underlying mechanisms are not yet understood. Experiments on vascular endothelial cells suggest that the electrical plasma membrane potential is involved in this regulatory process. To test this hypothesis we developed a technique that simultaneously measures the electrical membrane potential and stiffness of vascular endothelial cells (GM7373 cell line derived from bovine aortic endothelium) under continuous perfusion with physiological electrolyte solution. The cellular stiffness was determined by nano-indentation using an atomic force microscope (AFM) while the electrical membrane potential was measured with bis-oxonol, a voltage-reporting fluorescent dye. These two methods were combined using an AFM attached to an epifluorescence microscope. The electrical membrane potential and mechanical stiffness of the same cell were continuously recorded for a time span of 5 min. Fast fluctuations (in the range of seconds) of both the electrical membrane potential and mechanical stiffness could be observed that were not related to each other. In contrast, slow cell depolarizations (in the range of minutes) were paralleled by significant increases in mechanical stiffness. In conclusion, using the combined AFM–fluorescence technique we monitored for the first time simultaneously the electrical plasma membrane potential and mechanical stiffness in a living cell. Vascular endothelial cells exhibit oscillatory non-synchronized waves of electrical potential and mechanical stiffness. The sustained membrane depolarization, however, is paralleled by a concomitant increase of cell stiffness. The described method is applicable for any fluorophore, which opens new perspectives in biomedical research.



Visualization of membrane potential in bovine aortic endothelial cells by fluorescence microscopy; image 1 was obtained under basal conditions, while image 2 was obtained at maximal cell depolarization.

Biologically inspired rosette nanotubes and nanocrystalline hydroxyapatite hydrogel nanocomposites as improved bone substitutes

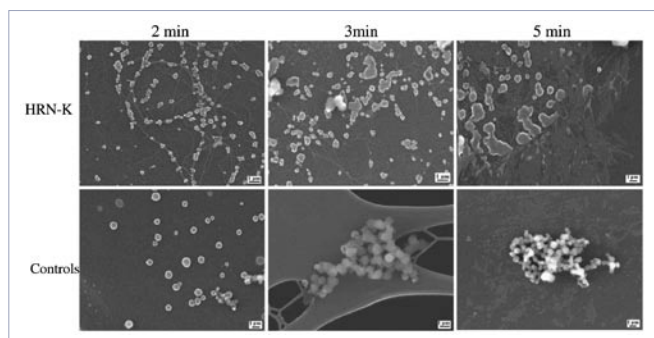
Lijie Zhang¹, Jose Rodriguez², Jose Raez², Andrew J Myles², Hicham Fenniri² and Thomas J Webster^{1,3,4}

¹ Division of Engineering, Brown University, 182 Hope Street, Providence, RI 02912, USA

² National Institute for Nanotechnology and Department of Chemistry, University of Alberta, 11421 Saskatchewan Drive, Edmonton, AB, T6G 2M9, Canada

³ Department of Orthopaedics, Brown University, Providence, RI 02818, USA

Today, bone diseases such as bone fractures, osteoporosis and bone cancer represent a common and significant public health problem. The design of biomimetic bone tissue engineering materials that could restore and improve damaged bone tissues provides exciting opportunities to solve the numerous problems associated with traditional orthopedic implants. Therefore, the objective of this *in vitro* study was to create a biomimetic orthopedic hydrogel nanocomposite based on the self-assembly properties of helical rosette nanotubes (HRNs), the osteoconductive properties of nanocrystalline hydroxyapatite (HA), and the biocompatible properties of hydrogels (specifically, poly(2-hydroxyethyl methacrylate), pHEMA). HRNs are self-assembled nanomaterials that are formed from synthetic DNA base analogs in water to mimic the helical nanostructure of collagen in bone. In this study, different geometries of nanocrystalline HA were controlled by either hydrothermal or sintering methods. 2 and 10 wt% nanocrystalline HA particles were well dispersed into HRN hydrogels using ultrasonication. The nanocrystalline HA and nanocrystalline HA/HRN hydrogels were characterized by x-ray diffraction, transmission electron microscopy, and scanning electron microscopy. Mechanical testing studies revealed that the well dispersed nanocrystalline HA in HRN hydrogels possessed improved mechanical properties compared to hydrogel controls. In addition, the results of this study provided the first evidence that the combination of either 2 or 10 wt% nanocrystalline HA and 0.01 mg ml⁻¹ HRNs in hydrogels greatly increased osteoblast (bone-forming cell) adhesion up to 236% compared to hydrogel controls. Moreover, this study showed that HRNs stimulated HA nucleation and mineralization along their main axis in a way that is very reminiscent of the HA/collagen assembly pattern in natural bone. In summary, the presently observed excellent properties of the biomimetic nanocrystalline HA/HRN hydrogel composites make them promising candidates for further study for bone tissue engineering applications.



SEM images of hydroxyapatite (HA) nucleation on helical rosette nanotubes (HRNs) and controls after incubation; after 2 min, HA formed and aligned on some HRNs compared to the random distributions of HA crystals on controls, and after 5 min, HA homogeneously covered most of the HRNs, while HA agglomeration occurred on controls.

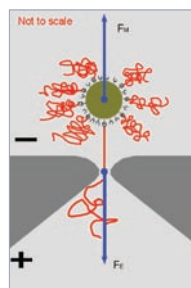
Reverse DNA translocation through a solid-state nanopore by magnetic tweezers

Hongbo Peng and Xinsheng Sean Ling

Department of Physics, Brown University, Providence, RI 02912, USA

Voltage-driven DNA translocation through nanopores has attracted wide interest for many potential applications in molecular biology and biotechnology. However, it is intrinsically difficult to control the DNA motion in standard DNA translocation processes in which a strong electric field is required in drawing DNA into the pore, but it also leads to uncontrollable fast DNA translocation. Here we explore a new type of DNA translocation.

We dub it 'reverse DNA translocation', in which the DNA is pulled through a nanopore mechanically by a magnetic bead, driven by a magnetic-field gradient. This technique is compatible with simultaneous ionic current measurements and is suitable for multiple nanopores, paving the way for large scale applications. We report the first experiment of reverse DNA translocation through a solid-state nanopore using magnetic tweezers.



Schematic of the reverse DNA translocation using magnetic tweezers; DNA (shown in red) is attached to the magnetic bead, and the electrical force on the DNA and magnetic force on the magnetic bead are drawn in blue.

AFM imaging of functionalized carbon nanotubes on biological membranes

C Lamprecht¹, I Liashkovich², V Neves³, J Danzberger¹, E Heister³, M Rangl¹, H M Coley³, J McFadden³, E Flahaut^{4,5}, H J Gruber¹, P Hinterdorfer¹, F Kienberger^{1,6} and A Ebner¹

¹ Institute of Biophysics, J Kepler University, Altenberger Straße 69, 4040 Linz, Austria

² Department of Physiology, University of Wuerzburg, 97070 Wuerzburg, Germany

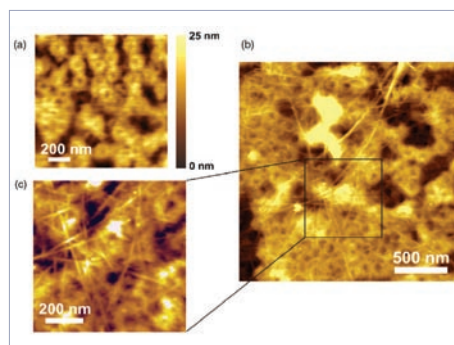
³ Faculty of Health and Medical Sciences, University of Surrey, Guildford GU2 7XH, UK

⁴ CNRS, Institut Carnot Cirimat, 31062 Toulouse, France

⁵ Université de Toulouse, UPS, INP, Institut Carnot Cirimat, 118, route de Narbonne, 31062 Toulouse cedex 9, France

⁶ Agilent Laboratories Linz, Aubrunnerweg 11, 4040 Linz, Austria

Multifunctional carbon nanotubes are promising for biomedical applications as their nano-size, together with their physical stability, gives access into the cell and various cellular compartments including the nucleus. However, the direct and label-free detection of carbon nanotube uptake into cells is a challenging task. The atomic force microscope (AFM) is capable of resolving details of cellular surfaces at the nanometer scale and thus allows following of the docking of carbon nanotubes to biological membranes. Here we present topographical AFM images of non-covalently functionalized single walled (SWNT) and double walled carbon nanotubes (DWNT) immobilized on different biological membranes, such as plasma membranes and nuclear envelopes, as well as on a monolayer of avidin molecules. We were able to visualize DWNT on the nuclear membrane while at the same time resolving individual nuclear pore complexes. Furthermore, we succeeded in localizing individual SWNT at the border of incubated cells and in identifying bundles of DWNT on cell surfaces by AFM imaging.



Topographic AFM images of the cytoplasmic side of the nuclear membrane; part (a) shows the typical ring structures of the nuclear pore complexes (NPCs) embedded in the nuclear membrane, parts (b) and (c) show the nuclear membrane covered with a net of RNA-coated DWNT lying across the NPCs.

ELECTRONICS AND PHOTONICS

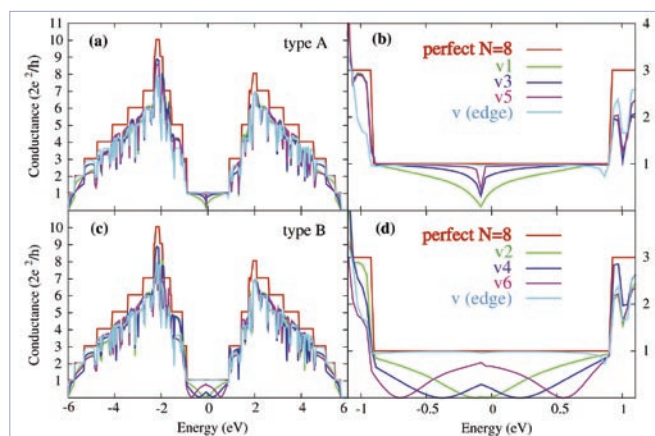
The effects of defects on the conductance of graphene nanoribbons

Narjes Gorjizadeh¹, Amir A Farajian² and Yoshiyuki Kawazoe¹

¹ Institute for Materials Research, Tohoku University, Sendai 980-8577, Japan

² Department of Mechanical and Materials Engineering, Wright State University, Dayton, OH 45435, USA

The quantum conductance of graphene nanoribbons that include vacancy and adatom–vacancy defects is studied for both armchair and zigzag edge structures. The conductance is calculated by using the Green's function formalism combined with a tight-binding method for the description of the system. Our results reveal that, owing to the localized states that appear near the defect sites, the conductance of the defected nanoribbons generally decreases. We show that details of the conductance reduction depend on the structure of the defect, its distance from the ribbon edges, and the ribbon width. While some defect structures cause the conductance of the ribbon to vanish, some other defects have no effect on the conductance at the Fermi energy.



Conductance of a zigzag-edge ribbon of graphene with vacancy defects. The details of the conductance reduction depend on the structure of the defect, its distance from the ribbon edges, and the ribbon width.

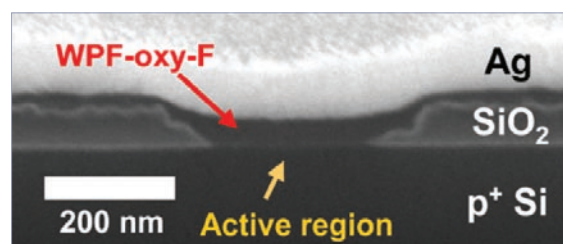
Resistive switching characteristics of polymer non-volatile memory devices in a scalable via-hole structure

Tae-Wook Kim, Hyejung Choi, Seung-Hwan Oh, Minseok Jo, Gunuk Wang, Byungjin Cho, Dong-Yu Kim, Hyunsang Hwang and Takhee Lee

Heeger Center for Advanced Materials, Department of Materials Science and Engineering, Gwangju Institute of Science and Technology, Gwangju 500-712, Korea

The resistive switching characteristics of polyfluorene-derivative polymer material in a sub-micron scale via-hole device structure were investigated. The scalable via-hole sub-microstructure was fabricated using an e-beam lithographic technique. The polymer non-volatile memory devices varied in size from $40 \times 40 \mu\text{m}^2$ to $200 \times 200 \text{nm}^2$. From the scaling of junction size, the memory mechanism can be attributed to the space-charge-limited

current with filamentary conduction. Sub-micron scale polymer memory devices showed excellent resistive switching behaviours such as a large ON/OFF ratio ($I_{\text{ON}}/I_{\text{OFF}} \sim 10^4$), excellent device-to-device switching uniformity, good sweep endurance, and good retention times (more than 10 000 s). The successful operation of sub-micron scale memory devices of our polyfluorene-derivative polymer shows promise to fabricate high-density polymer memory devices.



Scanning electron microscope image of a tilt view of a via-hole polymer non-volatile memory device. The high-performance resistive switching characteristics of these devices demonstrate the potential of their scalability in high-density memory devices.

Ordered polythiophene/fullerene composite core-shell nanorod arrays for solar cell applications

Featured on
nanotechweb.org

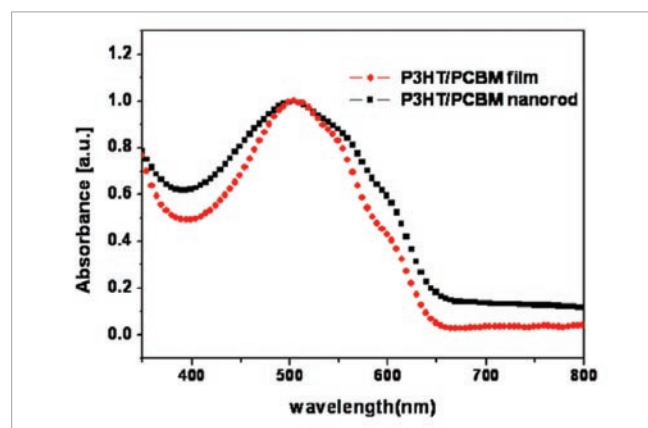
Hsu-Shen Wang¹, Li-Hua Lin¹, Shih-Yung Chen², Yuh-Lin Wang^{2,3} and Kung-Hwa Wei¹

¹ Department of Materials Science and Engineering, National Chiao Tung University, 1001 Ta Hsueh Road, Hsinch 30050, Taiwan, Republic of China

² Institute of Atomic and Molecular Science, Academia Sinica, PO Box 23-166, Taipei 106, Taiwan, Republic of China

³ Department of Physics, National Taiwan University, Taipei 106, Taiwan, Republic of China

For the first time, we have used melt-assisted wetting of porous alumina templates to prepare ordered core-shell nanorod arrays of poly(3-hexylthiophene) (P3HT) and [6,6]-phenyl-C61-butyric acid methyl ester (PCBM) for use in polymer solar cells. We characterized these arrays using tunneling electron microscopy and conductance atomic force microscopy, which revealed the presence of phase-separated shell (p-type) and core (n-type) regions. Under illumination, we observed a variation of several picoamperes between the currents in the core and shell regions of the P3HT/PCBM nanorod arrays.



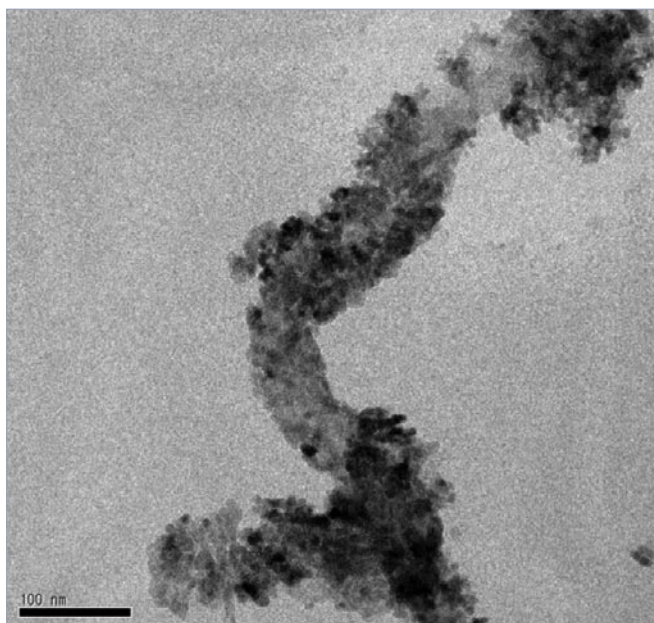
Scanning electron microscope images of the P3HT/PCBM nanorod nanostructures. The nanostructures have potential for use in efficient polymer solar cells.

Flexible photovoltaic cells fabricated utilizing ZnO quantum dot/carbon nanotube heterojunctions

Fushan Li, Dong Ick Son, Sung Hwan Cho, Won Tae Kim and Tae Whan Kim

National Research Laboratory for Nano Quantum Electronics, Division of Electronics and Computer Engineering, Hanyang University, 17 Haengdang-dong, Seongdong-gu, Seoul 133-791, Korea

In situ growth of ZnO quantum dots (QDs) on the surface of multi-walled carbon nanotubes (MWCNTs) was presented, and their application in photovoltaic cells by using flexible polyethylene terephthalate substrates was demonstrated. High-resolution transmission electron microscopy images revealed the conjugation of ZnO QDs with MWCNTs. Photoluminescence spectra indicated that the charge transfer efficiency at ZnO QD–MWCNT heterojunctions was above 90%, as confirmed by time-resolved photoluminescence measurements. Current–voltage measurements on the flexible devices fabricated utilizing ZnO QD–MWCNT heterojunctions showed the robust nature of the ZnO QD–MWCNT-based photovoltaic cells and their potential applications as the power source for flexible hand-held consumer electronics.



High-resolution transmission electron microscope image of an individual multi-walled carbon nanotube with ZnO quantum dots grown on the surface *in situ*. The charge transfer efficiency at the heterojunctions between the nanotube and quantum dots was above 90%.

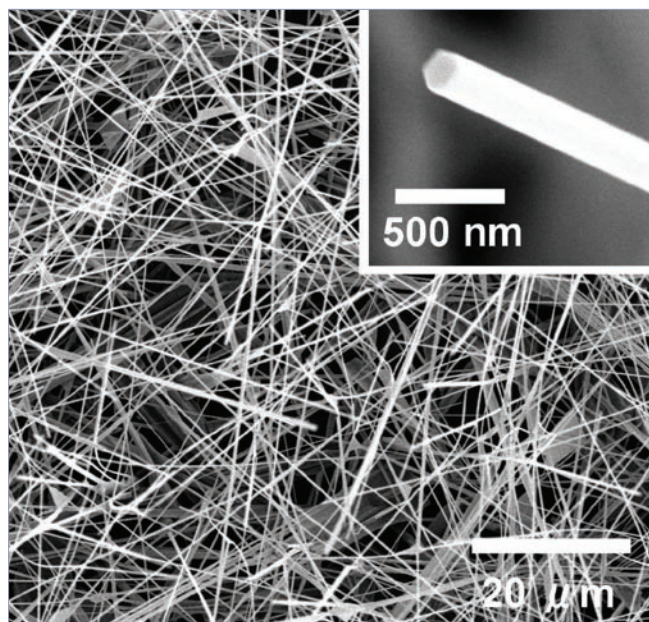
Electrical properties of individual ZnO nanowires

M Sakurai¹, Y G Wang¹, T Uemura² and M Aono¹

¹ International Center for Materials Nanoarchitectonics (MANA), National Institute for Materials Science (NIMS), Tsukuba 305-0044, Japan

² Graduate School of Science, Osaka University, Toyonaka 560-0043, Japan

The electrical properties of individual ZnO nanowires were investigated for two methods of fabricating nanowire–electrode junctions. The number of carriers in the nanowires was increased by electrostatically doping them by applying a gate voltage. The nanowires were chemically doped by introducing impurities during growth. The Ga-doped nanowires had a linear current–voltage relationship over a wide voltage region. The nanowire–electrode junctions were formed either by using lithography to form electrodes on the nanowire or by using an AFM probe to move a nanowire onto prepared electrodes. With both methods, electrodes made of Ga-doped ZnO were found to make better electrical contact with the nanowire than those made of Ti/Au.



Scanning electron microscopy image of ZnO nanowires grown on oxidized silicon substrate. Electrodes made of gallium-doped ZnO were found to make better electrical contact with the nanowire than those made of Ti/Au.

Did you know?

Nanotechnology received over 16,000 citations in 2008.

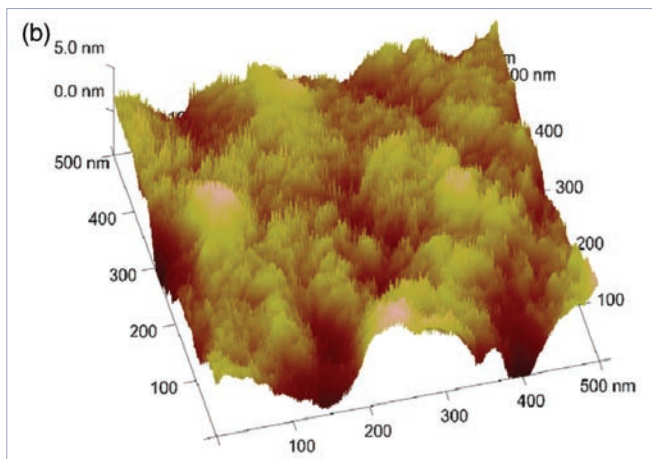
High efficiency polymer solar cells with vertically modulated nanoscale morphology

Ankit Kumar¹, Gang Li², Ziruo Hong¹ and Yang Yang^{1,2}

¹ Department of Material Science and Engineering, University of California, Los Angeles, CA 90095, USA

² Solarm Energy Incorporated, El Monte, CA 91731, USA

Nanoscale morphology has been shown to be a critical parameter governing charge transport properties of polymer bulk heterojunction (BHJ) solar cells. Recent results on vertical phase separation have intensified the research on 3D morphology control. In this paper, we intend to modify the distribution of donors and acceptors in a classical BHJ polymer solar cell by making the active layer richer in donors and acceptors near the anode and cathode respectively. Here, we chose [6,6]-phenyl-C61-butyric acid methyl ester (PCBM) to be the acceptor material to be thermally deposited on top of [poly(3-hexylthiophene)] P3HT: the PCBM active layer to achieve a vertical composition gradient in the BHJ structure. Here we report on a solar cell with enhanced power conversion efficiency of 4.5% which can be directly correlated with the decrease in series resistance of the device.



An annealed layer of [6,6]-phenyl-C61-butyric acid methyl ester. By fabricating a bulk heterojunction structure with a vertical composition gradient in the BHJ structure, the power conversion efficiency of the solar cell can be enhanced to 4.5%.

PATTERNING AND NANOFABRICATION

Surface-plasmon-enhanced fluorescence from periodic quantum dot arrays through distance control using biomolecular linkers

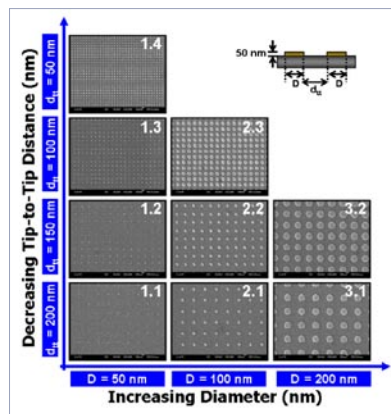
Melvin T Zin^{1,2}, Kirsty Leong³, Ngo-Yin Wong¹, Hong Ma¹, Mehmet Sarikaya¹ and Alex K-Y Jen^{1,3}

¹ Department of Materials Science and Engineering, University of Washington, Seattle, WA 98195, USA

² 3M Corporate Research Analytical Laboratory, 3M Center, St Paul, MN 55144, USA

³ Department of Chemistry, University of Washington, Seattle, WA 98195, USA

We have developed a protein-enabled strategy to fabricate quantum dot (QD) nanoarrays where up to a 15-fold increase in surface-plasmon-enhanced fluorescence has been achieved. This approach permits a comprehensive control both laterally (via lithographically defined gold nanoarrays) and vertically (via the QD-metal distance) of the collectively behaving assemblies of QDs and gold nanoarrays by way of biomolecular recognition. Specifically, we demonstrated the spectral tuning of plasmon resonant metal nanoarrays and self-assembly of protein-functionalized QDs in a stepwise fashion with a concomitant incremental increase in separation from the metal surface through biotin-streptavidin spacer units.



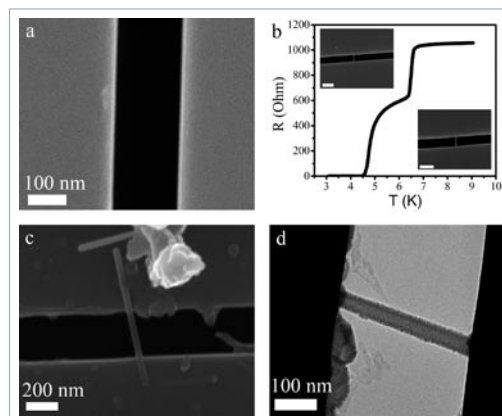
Dark-field images of gold nanoarrays. Precision control of the size and interspacing of the gold nanopillars leads to metal nanoarrays with distinct light scattering properties.

Nanoslits in silicon chips

Thomas Aref, Matthew Brenner and Alexey Bezyadin

Department of Physics, University of Illinois at Urbana-Champaign, 1110 West Green Street, Urbana, IL 61801, USA

Potassium hydroxide (KOH) etching of a patterned <100> oriented silicon wafer produces V-shaped etch pits. We demonstrate that the remaining thickness of silicon at the tip of the etch pit can be reduced to ~5 μm using an appropriately sized etch mask and optical feedback. Starting from such an etched chip, we have developed two different routes for fabricating 100 nm scale slits that penetrate through the macroscopic silicon chip (the slits are ~850 μm wide at one face of the chip and gradually narrow to ~100–200 nm wide at the opposite face of the chip). In the first process, the etched chips are sonicated to break the thin silicon at the tip of the etch pit and then further KOH etched to form a narrow slit. In the second process, focused ion beam milling is used to etch through the thin silicon at the tip of the etch pit. The first method has the advantage that it uses only low-resolution technology while the second method offers more control over the length and width of the slit. Our slits can be used for preparing mechanically stable, transmission electron microscopy samples compatible with electrical transport measurements or as nanostencils for depositing nanowires seamlessly connected to their contact pads.



A MoGe coated multi-walled nanotube spanning a transmission electron microscopy compatible slit milled by a focused ion beam.

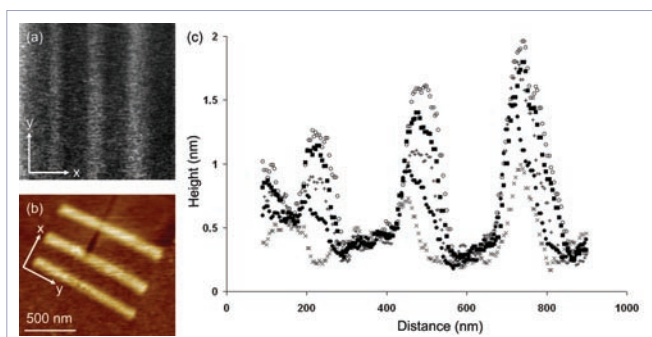
Real-time nanofabrication with high-speed atomic force microscopy

Featured on
nanotechweb.org

J A Vicary and M J Miles

H H Wills Physics Laboratory, University of Bristol, Tyndall Avenue, Bristol BS8 1TL, UK

The ability to follow nanoscale processes in real-time has obvious benefits for the future of material science. In particular, the ability to evaluate the success of fabrication processes *in situ* would be an advantage for many in the semiconductor industry. We report on the application of a previously described high-speed atomic force microscope (AFM) for nanofabrication. The specific fabrication method presented here concerns the modification of a silicon surface by locally oxidizing the region in the vicinity of the AFM tip. Oxide features were fabricated during imaging, with relative tip-sample velocities of up to 10 cm s^{-1} , and with a data capture rate of 15 fps.



High-speed atomic force microscopy images of three oxide lines. The frames were captured in 33 ms.

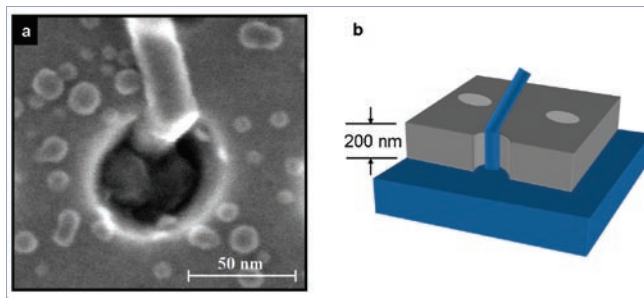
Guiding vapor-liquid-solid nanowire growth using SiO_2

Featured on
nanotechweb.org

Nathaniel J Quitoriano, Wei Wu and Theodore I Kamins

Information and Quantum Systems Laboratory, Hewlett-Packard Laboratories, Palo Alto, CA 94304, USA

Vapor-liquid-solid (VLS) grown nanowires (NWs) typically grow in $\langle 111 \rangle$ directions. In this work, using guiding structures, we effectively grow Si NWs with diameters between 20 and 100 nm in both $[001]$ and $\langle 110 \rangle$ directions by guiding the Si NW growth using SiO_2 surfaces. Using one structure, we demonstrate NW growth in the substrate plane, against the buried oxide layer of a standard, (001) silicon-on-insulator wafer. Using the other structure, we demonstrate NW growth perpendicular to a (001) substrate. We show that the VLS growth mechanism is the same as unconstrained NW growth, with the NWs still growing by the addition of $\{111\}$ planes. We show that when the guiding surface is removed, the NW grows in its natural growth direction because the growth mechanism has not changed. We speculate that NW growth can be guided with a range of materials, the most suitable being those that are amorphous and those which are nearly immiscible both with the catalyst and with the NW material.



Plan-view, scanning-electron micrograph SiO_2 with a hole about 50 nm in diameter and a silicon nanowire growing through it. Once the nanowire grows above the guiding oxide material, it changes growth direction.

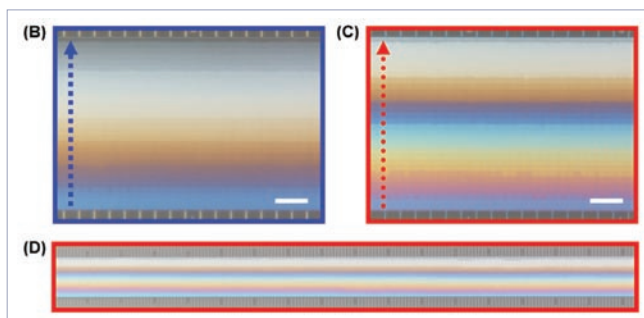
Nanofluidic structures with complex three-dimensional surfaces

Samuel M Stavis¹, Elizabeth A Strychalski² and Michael Gaitan¹

¹ Semiconductor Electronics Division, National Institute of Standards and Technology, Gaithersburg, MD 20899, USA

² Department of Physics, Cornell University, Ithaca, NY 14853, USA

Nanofluidic devices have typically explored a design space of patterns limited by a single nanoscale structure depth. A method is presented here for fabricating nanofluidic structures with complex three-dimensional (3D) surfaces, utilizing a single layer of grayscale photolithography and standard integrated circuit manufacturing tools. This method is applied to construct nanofluidic devices with numerous (30) structure depths controlled from ≈ 10 to ≈ 620 nm with an average standard deviation of < 10 nm over distances of > 1 cm. A prototype 3D nanofluidic device is demonstrated that implements size exclusion of rigid nanoparticles and variable nanoscale confinement and deformation of biomolecules.



Fluorescence micrograph of bacteriophage λ DNA molecules in the same nanofluidic structure. The DNA molecule assumed qualitatively different conformations as a function of depth and confinement in the structure.

Did you know?

That over 1,000,000 *Nanotechnology* articles were downloaded in 2008.

The fabrication of ZnO nanowire field-effect transistors by roll-transfer printing

Featured on
nanotechweb.org

Yi-Kuei Chang¹ and Franklin Chau-Nan Hong^{1,2,3}

¹ Department of Chemical Engineering, National Cheng Kung University, 1 University Road, Tainan 70101, Taiwan, Republic of China

² Center for Micro/Nano Science and Technology, National Cheng Kung University, 1 University Road, Tainan 70101, Taiwan, Republic of China

³ Advanced Optoelectronic Technology Center, National Cheng Kung University, 1 University Road, Tainan 70101, Taiwan, Republic of China

A method with the potential to fabricate large-area nanowire field-effect transistors (NW-FETs) was demonstrated in this study. Using a high-speed roller (20–80 cm min⁻¹), transfer printing was successfully employed to transfer vertically aligned zinc oxide (ZnO) nanowires grown on a donor substrate to a polydimethylsiloxane (PDMS) stamp and then print the ordered ZnO nanowire arrays on the received substrate for the fabrication of NW-FETs. ZnO NW-FETs fabricated by this method exhibit high performances with a threshold voltage of around 0.25 V, a current on/off ratio as high as 10⁵, a subthreshold slope of 360 mV/dec, and a field-effect mobility of around 90 cm² V⁻¹ s⁻¹. The excellent device characteristics suggest that the roll-transfer printing technique, which is compatible with the roll-to-roll (R2R) process and operated in atmosphere, has a good potential for the high-speed fabrication of large-area nanowire transistors for flexible devices and flat panel displays.



Scanning electron micrograph images of roll-transferred ZnO nanowires. Source and drain electrodes are deposited following the transfer.

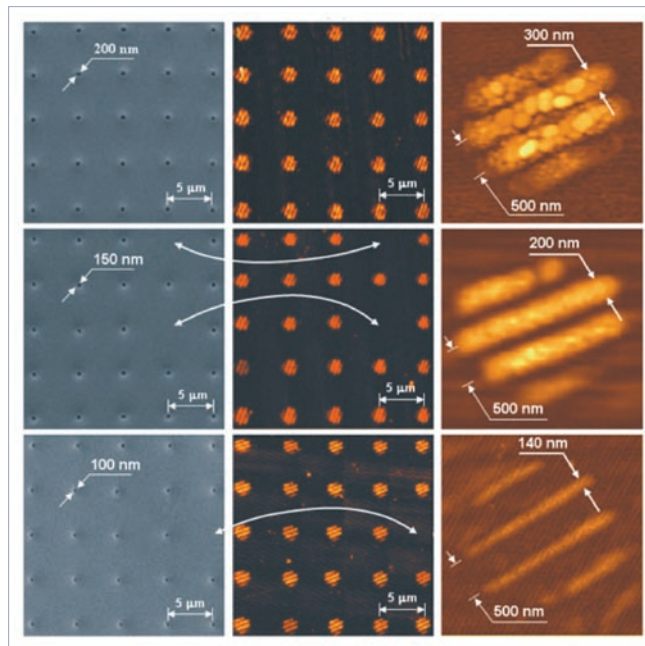
Nanolithography based on an atom pinhole camera

P N Melentiev¹, A V Zablotskiy², D A Lapshin¹, E P Sheshin², A S Baturin² and V I Balykin¹

¹ Institute of Spectroscopy, Russian Academy of Sciences, Troitsk, Moscow Region, Russia

² Moscow Institute of Physics and Technology, Dolgoprudniy, Moscow Region, Russia

In modern experimental physics the pinhole camera is used when the creation of a focusing element (lens) is difficult. We have experimentally realized a method of image construction in atom optics, based on the idea of an optical pinhole camera. With the use of an atom pinhole camera we have built an array of identical arbitrary-shaped atomic nanostructures with the minimum size of an individual nanostructure element down to 30 nm on an Si surface. The possibility of 30 nm lithography by means of atoms, molecules and clusters has been shown.



Scanning electron micrograph of membranes with nano-apertures with a diameter of 50 nm. The atom pinhole camera can be used for nanolithography with potential in the development of metamaterials, calibrating nanostructures for metrological problems, elements for plasmonics, spintronics, micro- and nanoelectromechanical systems and bionanosensors.

Nanopost plasmonic crystals

TT Truong^{1,2,3}, J Maria^{1,2,3}, J Yao^{1,2,3}, M E Stewart^{1,2,3}, T-W Lee⁴, S K Gray⁵, R G Nuzzo^{1,2,3} and J A Rogers^{1,2,3}

¹ Department of Materials Science and Engineering, University of Illinois at Urbana-Champaign, Urbana, IL 61801, USA

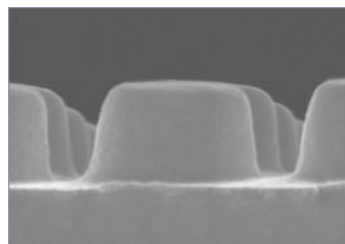
² Frederick Seitz Materials Research Laboratory, University of Illinois at Urbana-Champaign, Urbana, IL 61801, USA

³ Department of Chemistry, University of Illinois at Urbana-Champaign, Urbana, IL 61801, USA

⁴ Center for Computation and Technology, Louisiana State University, Baton Rouge, LA 70803, USA

⁵ Chemistry Division and Center for Nanoscale Materials, Argonne National Laboratory, Argonne, IL 60439, USA

We describe a class of plasmonic crystal that consists of square arrays of nanoposts formed by soft nanoimprint lithography. As sensors, these structure show somewhat higher bulk refractive index sensitivity for aqueous solutions in the visible wavelength range as compared to plasmonic crystals consisting of square arrays of nanowells with similar dimensions, with opposite trends for the case of surface bound layers in air. Three-dimensional finite-difference time-domain simulations quantitatively capture the key features and assist in the interpretation of these and related results.



Scanning electron micrograph of a plasmonic crystal. Results from experiment and modeling data suggest that nanopost and nanowell crystals might offer complementary advantages in biosensing and imaging with visible light.

QUANTUM PHENOMENA

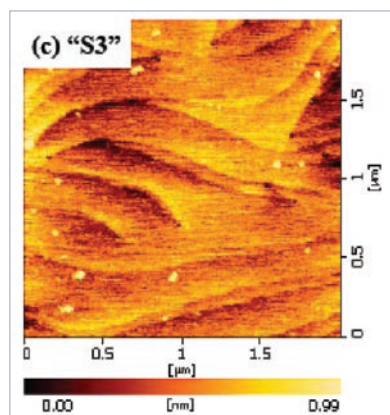
An InGaN/GaN single quantum well improved by surface modification of GaN films

Z L Fang^{1,3}, J Y Kang¹ and W Z Shen²

¹ Semiconductor Photonics Research Center and Department of Physics, Xiamen University, Xiamen 361005, People's Republic of China

² Department of Physics, Shanghai Jiao Tong University, Shanghai 200030, People's Republic of China

Surface modification of GaN films by *in situ* droplet homoepitaxy of thin GaN layers was employed for improvement of the surface/interface qualities characterized by atomic smoothness, low defect density and surface chemistry being close to stoichiometry. We find that, with surface modification of the GaN films the surface morphology of the subsequently grown InGaN/GaN single quantum well (SQW) was improved with less density of surface pits and indium-rich inclusions. The improvement in surface smoothness and InGaN/GaN surface/interface qualities is desirable for the growth of high-quality multiple QWs (MQWs) structures and fabrication of high-performance and reliable LEDs. PL results show that with surface modification the QW luminescence was significantly enhanced by more than 50% than that without surface modification.



The surface morphology of modified GaN film.

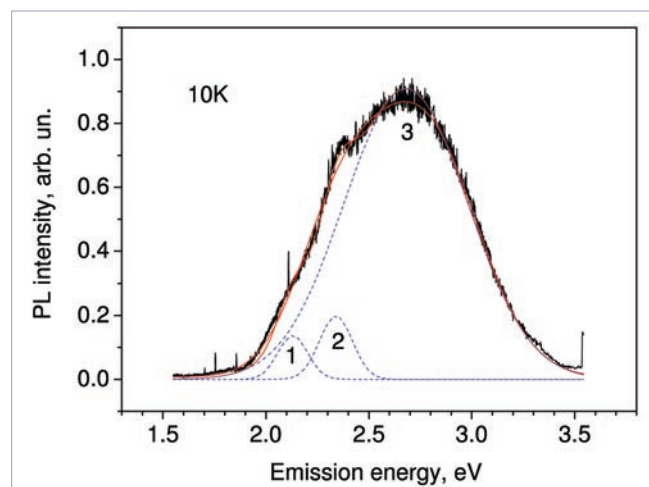
Interface states and bio-conjugation of CdSe/ZnS core-shell quantum dots

T V Torchynska

ESFM–Instituto Politécnico Nacional, México DF 07738, Mexico

The paper presents the results of photoluminescence (PL) and Raman scattering studies of non-conjugated and bio-conjugated CdSe/ZnS core-shell quantum dots (QDs). The commercial CdSe/ZnS QDs used are characterized by color emission with maxima at 605–610 nm (2.03–2.05 eV). PL spectra of non-conjugated QDs are the superposition of PL bands related to exciton emission in the CdSe core (2.03–2.05 eV) and to hot electron-hole emission via defect states at the CdSe/ZnS interface (2.37 and 2.68 eV). QD conjugation was performed with biomolecules—the antihuman interleukin 10 antibody (antihuman IL10). The PL spectra of bio-conjugated QDs have been changed dramatically: only one PL band related

to exciton emission in the CdSe core was detected in bio-conjugated QDs. To explain this effect a model has been proposed which assumes that the QD bio-conjugation process is accompanied by the recharging of acceptor-like interface states at the CdSe/ZnS interface. A comparative analysis of normalized PL spectra of non-conjugated CdSe/ZnS QDs with different intensities of interface state PL has confirmed the proposed electron-hole recombination model in QDs.



The photoluminescence spectrum for a quantum dot sample.

A fully coherent electron beam from a noble-metal covered W(111) single-atom emitter

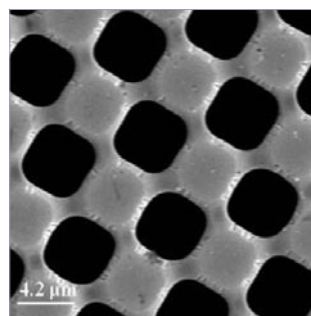
Featured on
nanotechweb.org

Che-Cheng Chang^{1,2}, Hong-Shi Kuo¹, Ing-Shouh Hwang^{1,2}, and Tien T Tsong¹

¹ Institute of Physics, Academia Sinica, Nankang, Taipei, Taiwan, Republic of China

² Department of Materials Science and Engineering, National Tsing Hua University, Hsinchu, Taiwan, Republic of China

In quantum mechanics, a wavefunction contains two factors: the amplitude and the phase. Only when the probing beam is fully phase coherent, can complete information be retrieved from a particle beam based experiment. Here we use the electron beam field emitted from a noble-metal covered W(111) single-atom tip to image single-walled carbon nanotubes (SWNTs) in an electron point projection microscope (PPM). The interference fringes of an SWNT bundle exhibit a very high contrast and the fringe pattern extends throughout the entire beam width. This indicates good phase correlation at all points transverse to the propagation direction. Application of these sources can significantly improve the performance and expand the capabilities of current electron beam based techniques. New instrumentation based on the full spatial coherence may allow determination of the three-dimensional atomic structures of nonperiodic nanostructures and make many advanced experiments possible.



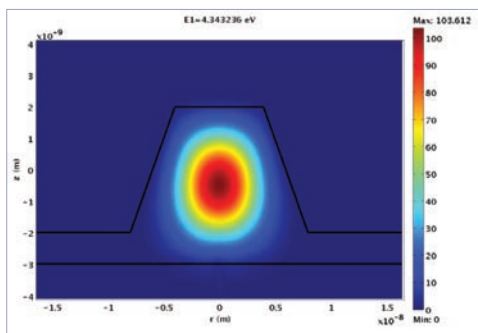
Secondary electron micrograph of part of a microfabricated Si₃N₄ membrane.

Thermoelectromechanical effects in quantum dots

Sunil R Patil and Roderick V N Melnik

M²NeT Laboratory, Wilfrid Laurier University, 75 University Avenue West, Waterloo, ON, N2L 3C5, Canada

Electromechanical effects are important in semiconductor nanostructures as most of the semiconductors are piezoelectric in nature. These nanostructures find applications in electronic and optoelectronic devices where they may face challenges for thermal management. Low dimensional semiconductor nanostructures, such as quantum dots (QD) and nanowires, are the nanostructures where such challenges must be particularly carefully addressed. In this contribution we report a study on thermoelectromechanical effects in QDs. For the first time a coupled model of thermoelectroelasticity has been applied to the analysis of quantum dots and the influence of thermoelectromechanical effects on bandstructures of low dimensional nanostructures has been quantified. Finite element solutions are obtained for different thermal loadings and their effects on the electromechanical properties and bandstructure of QDs are presented. Our model accounts for a practically important range of internal and external thermoelectromechanical loadings. Results are obtained for typical QD systems based on GaN/AlN and CdSe/CdS (as representatives of III–V and II–VI group semiconductors, respectively), with cylindrical and truncated conical geometries. The wetting layer effect on electromechanical quantities is also accounted for. The energy bandstructure calculations for various thermal loadings are performed. Electromechanical fields are observed to be more sensitive to thermal loadings in GaN/AlN QDs as compared to CdSe/CdS QDs. The results are discussed in the context of the effect of thermal loadings on the performance of QD-based nanosystems.



The influence of electromechanical effects on the bandstructure of truncated conical GaN/AlN quantum dots.

Thermal conductivity of carbon nanotubes with quantum correction via heat capacity

Michael C H Wu¹ and Jang-Yu Hsu^{1,2,3}

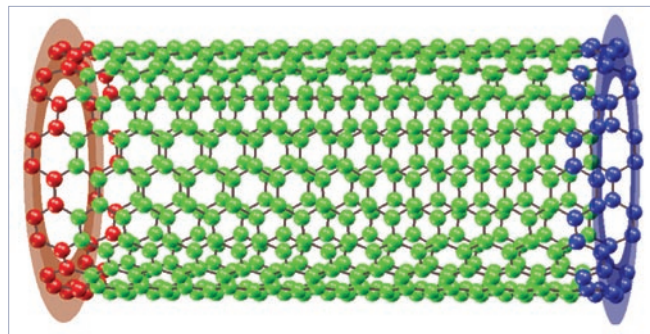
¹ Department of Physics, National Cheng Kung University, Tainan 701, Taiwan

² Institute of Space, Astrophysical and Plasma Sciences, National Cheng Kung University, Tainan 701, Taiwan

³ Department of Engineering and System Science, National Tsing Hua University, Hsinchu 30013, Taiwan

The molecular dynamics simulation with the use of the empirical Tersoff potential is applied to study the thermal characteristics of carbon nanotubes (CNTs). A thermal reservoir is devised to control the temperature and to exact the heat flux input. The quantum effect defining the precise temperature from the absolute zero Kelvin and up is included by applying phonon (boson) statistics to the specific heat. At low temperature, the

CNT thermal conductivity increases with increasing temperature. After reaching its peak, which is limited by the length of the CNT, it decreases with temperature due to phonon–phonon interactions. The scaling law of thermal conductivity as a function of temperature and length is inferred from the simulation results, allowing prediction for CNTs of much longer length beyond what MD could simulate.



A model of the thermal conductivity of an armchair CNT.

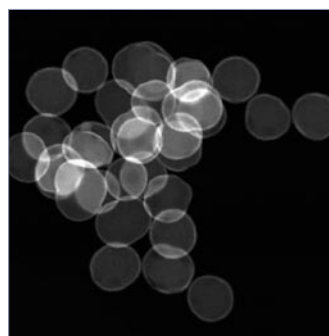
Atomic layer deposition of quantum-confined ZnO nanostructures

Featured on
nanotechweb.org

David M King, Samantha I Johnson, Jianhua Li, Xiaohua Du, Xinhua Liang and Alan W Weimer

Department of Chemical and Biological Engineering, University of Colorado, Boulder, CO 80309, USA

The modulation of optoelectronic properties, such as the bandgap of a pure-component semiconductor material, is a useful ability that can be achieved by few techniques. Atomic layer deposition (ALD) was used here to experimentally demonstrate the ability to deposit films that exhibit quantum confinement on three-dimensional surfaces. Polycrystalline ZnO films ranging from ~1.5 to 15 nm in thickness were deposited via ALD using diethylzinc and hydrogen peroxide at 100 °C. Conformal, pinhole-free films were deposited on Si wafers and on nanosized spherical SiO₂ particles using an augmented central composite design strategy. Powder x-ray diffraction was used to measure the crystallite size of the films and monitor size evolution on the basis of the number of ALD cycles and thermal annealing post-treatments. The absorbance of the ZnO films on Si wafers and SiO₂ particles was measured using spectroscopic ellipsometry and diffuse transmittance techniques, respectively. Post-deposition annealing steps increased the crystallite size of the films, independently of the coating thickness. The ZnO bandgap was increasingly blue-shifted for films of decreasing crystallite size, approaching +0.3 eV at dimensions of 2–3 nm. The nonlinear bandgap response correlated well with the Brus model. This work represents an experimental demonstration of quantum confinement using ALD on two- and three-dimensional substrates.



STEM image of conformal nanoscale ZnO ALD films on spherical SiO₂ nanoparticles.

**MATERIALS: SYNTHESIS OR
SELF-ASSEMBLY**

Hierarchically organized nanostructured TiO₂ for photocatalysis applications

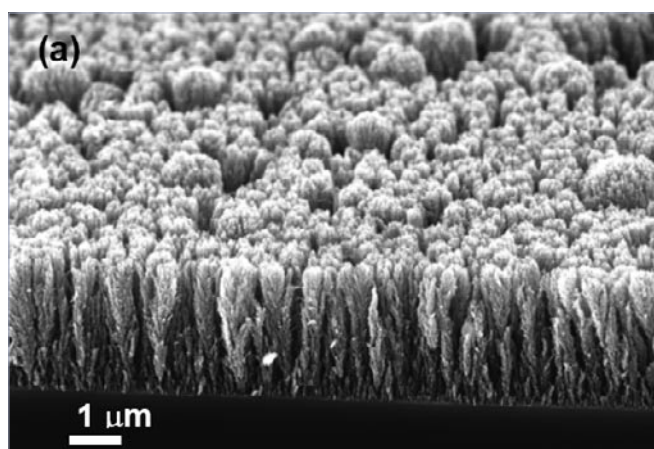
F Di Fonzo^{1,2}, C S Casari^{1,2}, V Russo^{1,2}, M F Brunella³, A Li Bassi^{1,2} and C E Bottani^{1,2}

¹ Politecnico di Milano, Dipartimento di Chimica, Materiali e Ingegneria Chimica 'G Natta', via Ponzio 34/3, 20133 Milano, Italy

² NEMAS—Center for NanoEngineered Materials and Surfaces, via Ponzio 34/3, 20133 Milano, Italy

³ Politecnico di Milano, Dipartimento di Chimica, Materiali e Ingegneria Chimica 'G Natta', via Mancinelli 7, 20131 Milano, Italy

A template-free process for the synthesis of nanocrystalline TiO₂ hierarchical microstructures by reactive pulsed laser deposition (PLD) is here presented. By a proper choice of deposition parameters a fine control over the morphology of TiO₂ microstructures is demonstrated, going from classical compact/columnar films to a dense forest of distinct hierarchical assemblies of ultrafine nanoparticles (<10 nm), up to a more disordered, aerogel-type structure. Correspondingly, the film density varies with respect to bulk TiO₂ anatase, with a degree of porosity going from 48% to over 90%. These structures are stable with respect to heat treatment at 400 °C, which results in crystalline ordering but not in morphological changes down to the nanoscale. Both as deposited and annealed films exhibit very promising photocatalytic properties, even superior to standard Degussa-P25 powder, as demonstrated by the degradation of stearic acid as a model molecule. The observed kinetics are correlated to the peculiar morphology of the PLD grown material. We show that the 3D multiscale hierarchical morphology enhances reaction kinetics and creates an ideal environment for mass transport and photon absorption, maximizing the surface area-to-volume ratio while at the same time providing readily accessible porosity through the large inter-tree spaces that act as distributing channels. The reported strategy provides a versatile technique to fabricate high aspect ratio 3D titania microstructures through a hierarchical assembly of ultrafine nanoparticles. Beyond photocatalytic and catalytic applications, this kind of material could be of interest for those applications where high surface-to-volume and efficient mass transport are required at the same time.



SEM image of nanoscale TiO₂ film deposited at 40 Pa.

Self-aligned growth of single-walled carbon nanotubes using optical near-field effects

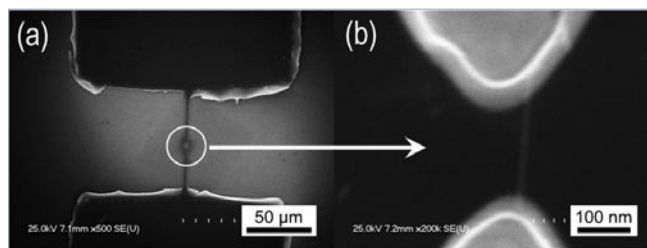
Featured on
nanotechweb.org

W Xiong¹, Y S Zhou¹, M Mahjouri-Samani¹, W Q Yang¹, K J Yi¹, X N He¹, S H Liou² and Y F Lu¹

¹ Department of Electrical Engineering, University of Nebraska-Lincoln, Lincoln, NE 68588-0511, USA

² Department of Physics and Astronomy, University of Nebraska-Lincoln, Lincoln, NE 68588-0111, USA

Self-aligned growth of ultra-short single-walled carbon nanotubes (SWNTs) was realized by utilizing optical near-field effects in a laser-assisted chemical vapor deposition (LCVD) process. By introducing the optical near-field effects, bridge structures containing single suspended SWNT channels were successfully fabricated through the LCVD process at a relatively low substrate temperature. Raman spectroscopy and *I*-*V* analyses have been carried out to characterize the SWNT-bridge structures. Numerical simulations using a high-frequency structure simulator revealed that significant enhancement of local heating occurs at metallic electrode tips under laser irradiation; it is about one order of magnitude higher than that in the rest of the electrodes. This technique suggests a novel approach to *in situ* low-temperature fabrication of SWNT-based devices in a precisely controlled manner, based on the nanoscale heating enhancement induced by the optical near-field effects.



SEM micrograph of SWNT-bridge structure.

Nanotechnology Special Issues in 2009

- Nanoscale phenomena in hydrogen storage
- High-resolution noncontact atomic force microscopy
- Invited articles celebrating the 20th volume of *Nanotechnology*

Photo-induced effects on self-organized TiO₂ nanotube arrays: the influence of surface morphology

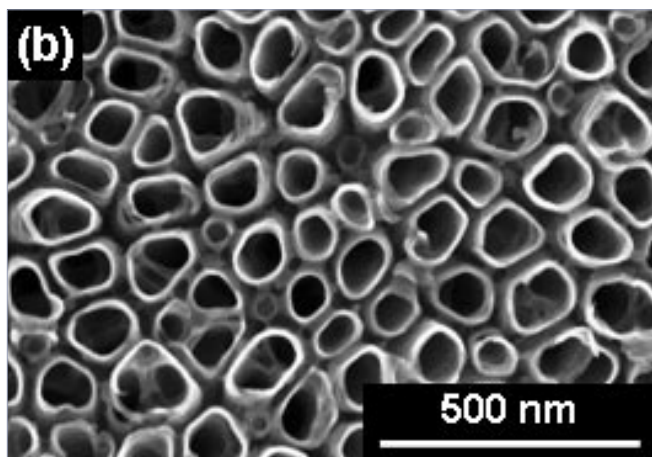
Featured on
nanotechweb.org

A G Kontos¹, A I Kontos¹, D S Tsoukleris¹, V Likodimos¹, J Kunze², P Schmuk² and P Falaras¹

¹ Institute of Physical Chemistry, NCSR 'Demokritos', 15310 Aghia Paraskevi Attikis, Athens, Greece

² Department of Materials Science and Engineering, WW4-LKO, University of Erlangen-Nuremberg, Martensstrasse 7 D-91058 Erlangen, Germany

Self-organized TiO₂ nanotubes with packed, vertically aligned morphology and different lateral characteristics were grown on Ti metal substrates by controlled electrochemical anodization in phosphate/HF and ethylene glycol/HF electrolytes. The wetting, photo-induced superhydrophilicity, and photocatalytic activity of the nanotubular materials were investigated under ultraviolet irradiation. The photoactivity of the TiO₂ nanotube arrays was analysed in terms of their morphological characteristics that were determined by means of scanning electron microscopy and atomic force microscopy in conjunction with geometrical modelling. The wetting and the UV-induced superhydrophilicity could be accordingly modelled by the Cassie–Baxter mode arising from the large scale roughness of the nanotubular arrays in combination with the Wenzel mode due to the small scale roughness induced by ridges at the outer tube surface. The photocatalytic activity of the TiO₂ nanotube arrays was further found to correlate quantitatively with the variation of the geometric roughness factor, verifying the strong impact of morphology on the photo-induced properties of the vertically oriented TiO₂ tubular architecture.



Top view SEM image of TiO₂ nanotubes.

Three-dimensional electrodes for dye-sensitized solar cells: synthesis of indium–tin-oxide nanowire arrays and ITO/TiO₂ core–shell nanowire arrays by electrophoretic deposition

Featured on
nanotechweb.org

Hong-Wen Wang¹, Chi-Feng Ting¹, Miao-Ken Hung¹, Chwei-Huann Chiou², Ying-Ling Liu³, Zongwen Liu⁴, Kyle R Ratinac⁴ and Simon P Ringer⁴

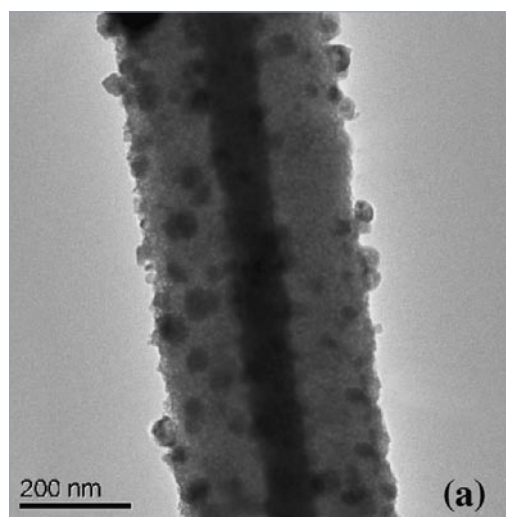
¹ Department of Chemistry, Center for Nanotechnology, Chung-Yuan Christian University, Chungli 320, Taiwan, Republic of China

² Chemical Engineering Division, Institute of Nuclear Energy Research, No. 1000, Wenhua Road Jiaan Village, Lungtan Township, Taoyuan County 32546, Taiwan, Republic of China

³ R&D Center for Membrane Technology, Chung-Yuan Christian University, Chungli 320, Taiwan, Republic of China

⁴ Australian Key Centre for Microscopy and Microanalysis, Electron Microscope Unit, University of Sydney, Sydney, NSW 2006, Australia

Dye-sensitized solar cells (DSSCs) show promise as a cheaper alternative to silicon-based photovoltaics for specialized applications, provided conversion efficiency can be maximized and production costs minimized. This study demonstrates that arrays of nanowires can be formed by wet-chemical methods for use as three-dimensional (3D) electrodes in DSSCs, thereby improving photoelectric conversion efficiency. Two approaches were employed to create the arrays of ITO (indium–tin-oxide) nanowires or arrays of ITO/TiO₂ core–shell nanowires; both methods were based on electrophoretic deposition (EPD) within a polycarbonate template. The 3D electrodes for solar cells were constructed by using a doctor-blade for coating TiO₂ layers onto the ITO or ITO/TiO₂ nanowire arrays. A photoelectric conversion efficiency as high as 4.3% was achieved in the DSSCs made from ITO nanowires; this performance was better than that of ITO/TiO₂ core–shell nanowires or pristine TiO₂ films. Cyclic voltammetry confirmed that the reaction current was significantly enhanced when a 3D ITO-nanowire electrode was used. Better separation of charge carriers and improved charge transport, due to the enlarged interfacial area, are thought to be the major advantages of using 3D nanowire electrodes for the optimization of DSSCs.



TEM micrograph of a single ITO/TiO₂ core-shell nanowire.

Spray deposition of steam treated and functionalized single-walled and multi-walled carbon nanotube films for supercapacitors

Featured on
nanotechweb.org

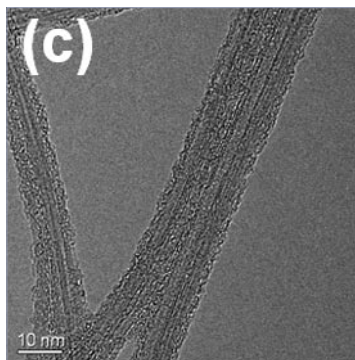
Xin Zhao¹, Bryan TT Chu¹, Belén Ballesteros², Weiliang Wang³, Colin Johnston¹, John M Sykes¹ and Patrick S Grant¹

¹ Department of Materials, Oxford University, Parks Road, Oxford OX1 3PH, UK

² Inorganic Chemistry Laboratory, Oxford University, South Parks Road, Oxford OX1 3QR, UK

³ Department of Engineering Science, Oxford University, Parks Road, Oxford OX1 3PJ, UK

Steam purified, carboxylic and ester functionalized single-walled carbon nanotube (SWNT) and multi-walled carbon nanotube (MWNT) films with homogeneous distribution and flexible control of thickness and area were fabricated on polymeric and metallic substrates using a modified spray deposition technique. By employing a pre-sprayed polyelectrolyte, the adhesion of the carbon nanotube (CNT) films to the substrates was significantly enhanced by electrostatic interaction. Carboxylic and ester functionalization improved electrochemical performance when immersed in 0.1 M H₂SO₄ and the specific capacitance reached 155 and 77 F g⁻¹ for carboxylic functionalized SWNT and MWNT films respectively. Compared with existing techniques such as hot pressing, vacuum filtration and dip coating, the ambient pressure spray deposition technique is suggested as particularly well suited for preparing CNT films at large scale for applications including providing electrodes for electrochemical supercapacitors and paper batteries.



HRTEM image of carboxylic functionalized single walled nanotubes.

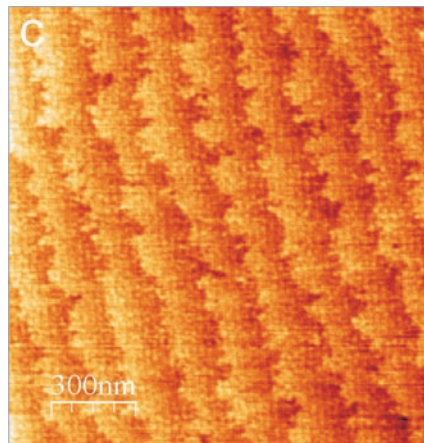
Graphene on insulating crystalline substrates

S Akçöltekin, M El Kharrazi, B Köhler, A Lorke and M Schleberger

Fachbereich Physik, CeNIDE, Universität Duisburg-Essen, D-47048 Duisburg, Germany

We show that it is possible to prepare and identify ultra-thin sheets of graphene on crystalline substrates such as SrTiO₃, TiO₂, Al₂O₃ and CaF₂ by standard techniques (mechanical exfoliation, optical and atomic force microscopy). On the substrates under consideration we find a similar distribution of single layer, bilayer and few-layer graphene and graphite flakes as with conventional SiO₂ substrates. The optical contrast C of a single graphene layer on any of those substrates is determined by

calculating the optical properties of a two-dimensional metallic sheet on the surface of a dielectric, which yields values between C = -1.5% (G/TiO₂) and C = -8.8% (G/CaF₂). This contrast is in reasonable agreement with experimental data and is sufficient to make identification by an optical microscope possible. The graphene layers cover the crystalline substrate in a carpet-like mode and the height of single layer graphene on any of the crystalline substrates as determined by atomic force microscopy is dSLG = 0.34 nm and thus much smaller than on SiO₂.



AFM image of the CaF₂ surface.

A novel method for metal oxide nanowire synthesis

Simas Rackauskas¹, Albert G Nasibulin¹, Hua Jiang¹, Ying Tian¹, Victor I Kleshch^{2,3}, Jani Sainio⁴, Elena D Obratsova², Sofia N Bokova², Alexander N Obratsov^{3,5} and Esko I Kauppinen^{1,6}

¹ NanoMaterials Group, Department of Applied Physics and Center for New Materials, Helsinki University of Technology, P.O.B 5100, FIN-02015, Espoo, Finland

² A M Prokhorov General Physics Institute of Russian Academy of Sciences, 38 Vavilov street, 119991, Moscow, Russia

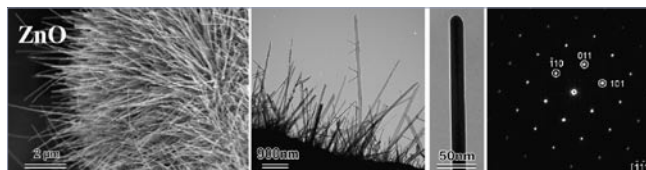
³ Physics Department of M V Lomonosov Moscow State University, Leninskie gory, 1, 119991, Moscow, Russia

⁴ Laboratory of Physics, Helsinki University of Technology, P.O.B 1100, FIN-02015, Espoo, Finland

⁵ University of Joensuu, P.O.B 111, FIN-80101, Joensuu, Finland

⁶ VTT Biotechnology, P.O.B 1000, FIN-02044, Espoo, Finland

Nanowires (NWs) of metal oxides (Fe₂O₃, CuO, V₂O₅ and ZnO) were grown by an efficient non-catalytic economically favorable method based on resistive heating of pure metal wires or foils at ambient conditions. The growth rate of iron oxide NWs exceeds 100 nm s⁻¹. Produced NWs were typically 1–5 μm long with diameters from 10 to 50 nm. The produced metal oxide NWs were characterized by means of SEM, TEM, EDX, XPS and Raman techniques. The field emission measurements from the as-produced CuO NWs were found to have a threshold field as low as 4 V μm⁻¹ at 0.01 mA cm⁻². The formation mechanism of the NWs is discussed.



Electron microscope images of V₂O₅ and ZnO nanowires.

Templated growth of graphenic materials

Nolan W Nicholas^{1,2}, L Matthew Connors¹, Feng Ding³, Boris I Yakobson⁴, Howard K Schmidt^{2,5} and Robert H Hauge^{2,6}

¹ Department of Physics, Rice University, 6100 Main, Houston, TX, USA

² Richard E Smalley Institute for Nanoscale Science and Technology, Rice University, 6100 Main, Houston, TX, USA

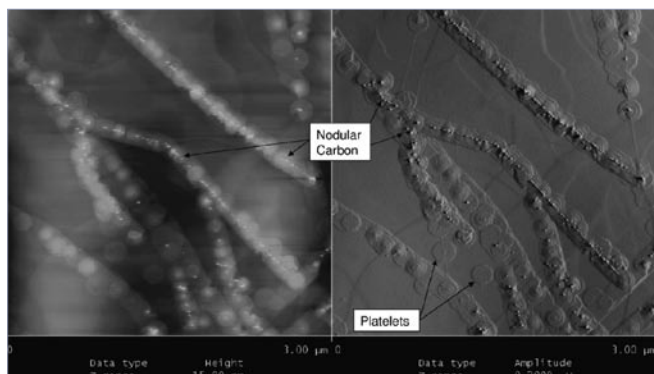
³ Institute of Textile and Clothing, Hong Kong Polytechnic University, Kowloon, Hong Kong

⁴ Department of Mechanical Engineering and Materials Science, Rice University, 6100 Main, Houston, TX, USA

⁵ Department of Chemical and Biomolecular Engineering, Rice University, 6100 Main, Houston, TX, USA

⁶ Department of Chemistry, Rice University, 6100 Main, Houston, TX, USA

A novel strategy is proposed for the topologically controlled synthesis of extended graphenic sheets by additively reacting carbon into a pre-existing graphene sheet which is on top of a templating substrate. This concept is implemented and demonstrated using chemical vapor deposition (CVD). Novel morphological features observed in this study suggest unusual aspects of the CVD growth process. CVD results demonstrate the basic soundness of the synthesis strategy but highlight the sensitivity of the process to certain types of disruption and the need for alternative forms of embodiment.



AFM image showing nodular carbon atop circular growth structures.

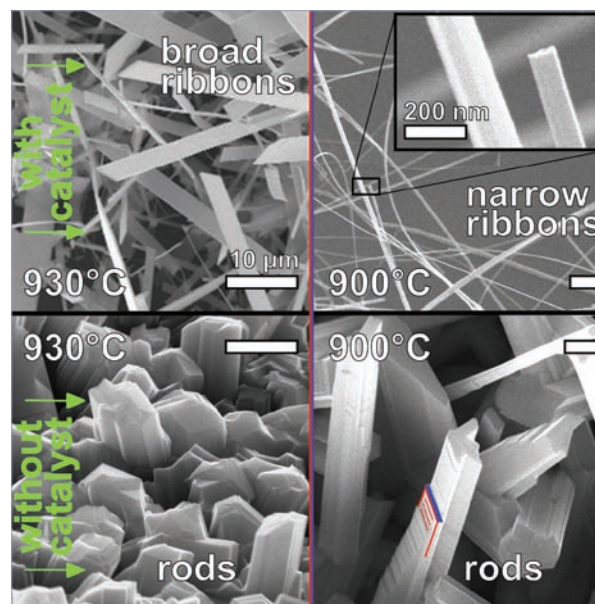
Ultrafast VLS growth of epitaxial β -Ga₂O₃ nanowires

E Auer¹, A Lugstein¹, S Löffler¹, Y J Hyun¹, W Brezna¹, E Bertagnoli¹ and P Pongratz²

¹ Institute for Solid State Electronics, Vienna University of Technology, Floragasse 7, A-1040 Vienna, Austria

² Institute for Solid State Physics, Vienna University of Technology, Wiedner Hauptstraße 8/052, A-1040 Vienna, Austria

Well-defined monoclinic nanostructures of β -Ga₂O₃ were grown in a chemical vapor deposition apparatus using metallic gallium and oxygen as sources. Stable growth conditions were deduced for nanorods, nanoribbons, nanowires and cones. The types of nanostructures are determined by the growth temperature. We suppose that the vapor–solid growth mechanism rules the growth of nanoribbons and rods. For the nanowires we observed catalytic gold droplets atop, characteristic for the VLS growth mechanism with an extremely high growth rate of up to 10 $\mu\text{m min}^{-1}$. Nanowires grown on Al₂O₃ substrates showed an excellent tendency to grow epitaxially, mapping the hexagonal symmetry of Al₂O₃(0001).



SEM images showing Ga₂O₃ nanostructures grown on thermal silicon oxide at different temperatures.

SENSING AND ACTUATING

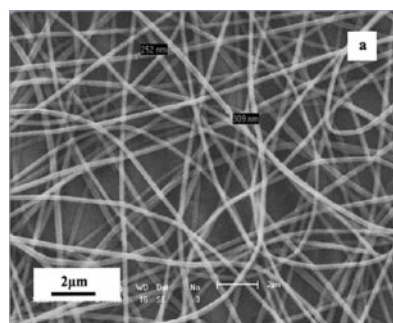
A highly sensitive ethanol sensor based on mesoporous ZnO–SnO₂ nanofibers

Xiaofeng Song¹, Zhaojie Wang¹, Yongben Liu¹, Ce Wang¹ and Lijuan Li²

¹ Alan G Macdiarmid Institute, Jilin University, Changchun 130012, People's Republic of China

² Department of Chemistry and Biochemistry, California State University, Long Beach, CA 90840, USA

A facile and versatile method for the large-scale synthesis of sensitive mesoporous ZnO–SnO₂ (m-Z-S) nanofibers through a combination of surfactant-directed assembly and an electrospinning approach is reported. The morphology and the structure were investigated by scanning electron microscopy (SEM), transmission electron microscopy (TEM), x-ray diffraction (XRD), and nitrogen adsorption–desorption isotherm analysis. The results showed that the diameters of fibers ranged from 100 to 150 nm with mixed structures of wurtzite (ZnO) and rutile (SnO₂), and a mesoporous structure was observed in the m-Z-S nanofibers. The sensor performance of the prepared m-Z-S nanofibers was measured for ethanol. It is found that the mesoporous fiber film obtained exhibited excellent ethanol sensing properties, such as high sensitivity, quick response and recovery, good reproducibility, and linearity in the range 3–500 ppm.



SEM images of mesoporous ZnO–SnO₂ precursor fibers.

Novel porous single-crystalline ZnO nanosheets fabricated by annealing ZnS(en)_{0.5} (en = ethylenediamine) precursor. Application in a gas sensor for indoor air contaminant detection

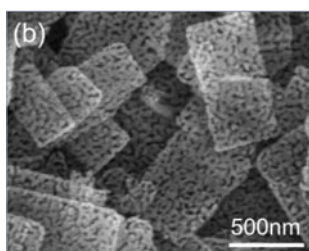
Featured on
nanotechweb.org

Jinyun Liu¹, Zheng Guo^{1,2}, Fanli Meng¹, Tao Luo¹, Minqiang Li¹ and Jinhui Liu¹

¹ The Key Laboratory of Biomimetic Sensing and Advanced Robot Technology, Hefei Institute of Intelligent Machines, Chinese Academy of Sciences, Hefei 230031, People's Republic of China

² Department of Chemistry, University of Science and Technology of China, Hefei 230026, People's Republic of China

Novel single-crystalline ZnO nanosheets with porous structure have been fabricated by annealing ZnS(en)_{0.5} (en = ethylenediamine) complex precursor. The morphology and structure observations performed by field emission scanning electronic microscopy (FESEM) and high-resolution transmission electron microscopy (HRTEM) indicate that numerous mesopores with a diameter of about 26.1 nm distribute all through each nanosheet with a high density. The transformation of structure and composition of samples obtained during thermal treatment processes were investigated by x-ray diffraction (XRD), x-ray photoelectron spectrometry (XPS), thermogravimetric analysis (TGA), and Fourier transform infrared (FTIR) absorption spectroscopy. The formation mechanism of the porous structure is proposed. For indoor air contaminant detection in which formaldehyde and ammonia are employed as target gases, the as-prepared ZnO nanosheets were applied for the fabrication of gas sensors. It was found that the as-fabricated sensors not only exhibit highly sensitive performance, e.g., high gas-sensing responses, short response and recovery time, but also possess significant long-term stability. It is indicated that these ZnO nanostructures could promisingly be applied in electronic devices for environmental evaluation.



A FESEM image of the as-synthesized complex precursor and porous products.

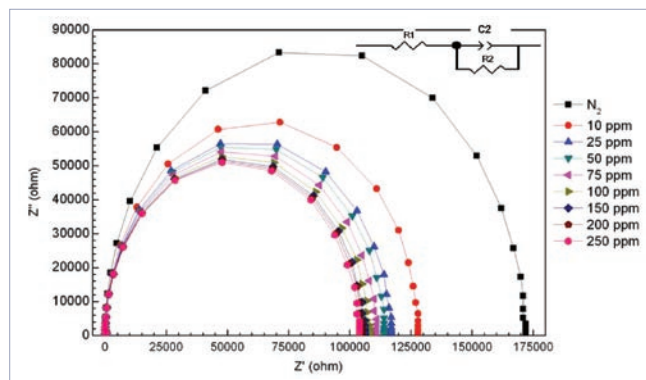
Carbon nanotube-based ethanol sensors

Sean Brahim, Steve Colbern, Robert Gump, Alex Moser and Leonid Grigorian

YTC America Incorporated, Camarillo, CA 93012, USA

Sensors containing metal-carbon nanotube (CNT) hybrid materials as the active sensing layer were demonstrated for ethanol vapor detection at room temperature. The metal-CNT hybrid materials were synthesized by infiltrating single wall carbon nanotubes (SWNTs) with the transition metals Ti, Mn, Fe, Co, Ni, Pd or Pt. Each sensor was prepared by drop-casting dilute

dispersions of a metal-CNT hybrid onto quartz substrate electrodes and the impedimetric responses to varying ethanol concentration were recorded. Upon exposure to ethanol vapor, the ac impedance (Z') of the sensors was found to decrease to different extents. The sensor containing pristine CNT material was virtually non-responsive at low ethanol concentrations (<50 ppm). In contrast, all metal-CNT hybrid sensors showed extremely high sensitivity to trace ethanol levels with 100-fold or more gains in sensitivity relative to the starting SWNT sensor. All hybrid sensors, with the exception of Ni filled CNT, exhibited significantly larger sensor responses to ethanol vapor up to 250 ppm compared to the starting SWNT sensor.



Characteristic Nyquist plots observed for the Fe infiltrated CNT hybrid sensor in response to various concentrations of ethanol vapor.

Non-functionalized silver nanoparticles for a localized surface plasmon resonance-based glucose sensor

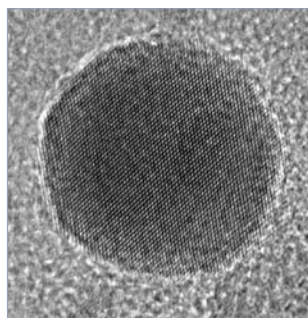
A Serra¹, E Filippo¹, M Re², M Palmisano², M Vittori-Antisari³, A Buccolieri¹ and D Manno¹

¹ Dipartimento di Scienza dei Materiali, Università del Salento, Via Monteroni, 73100 Lecce, Italy

² ENEA-Centro Ricerche Brindisi, S S Appia-km 706, 72100 Brindisi, Italy

³ ENEA-Centro Ricerche Casaccia, via Anguillarese, 301, 00123 Santa Maria di Galeria, Roma, Italy

The optical properties of non-functionalized silver nanoparticles in ethanol solution have been analyzed and a progressive shift of localized surface plasmon resonances caused by the adding of increasing quantities of glucose has been observed. To understand this occurrence, the interaction of glucose molecules with the silver nanoparticle surface has been investigated using Raman spectroscopy. In addition, high resolution transmission electron microscopy shows the presence of superstructures on the silver nanoparticle surface that can be imputed to the presence of glucose.



A HRTEM image obtained from a silver particle coming from a pure silver colloidal dispersion and a silver particle.

A new multifunctional platform based on high aspect ratio interdigitated NEMS structures

Featured on
nanotechweb.org

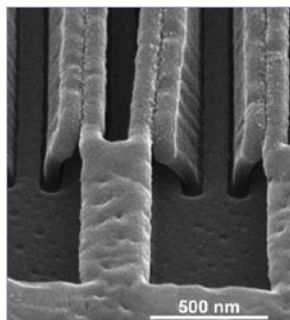
S Ghatnekar-Nilsson¹, I Karlsson¹, A Kvennefors^{1,2}, G Luo^{1,2}, V Zela¹, M Arlelid³, T Parker¹, L Montelius² and A Litwin¹

¹ NEMS AB, Solvegatan 16, S-223 62 Lund, Sweden

² Solid State Physics/The Nanometer Structure Consortium, Lund University, PO Box 118, S-221 00 Lund, Sweden

³ Electrical and Information Technology, Lund University, PO Box 118, S-221 00 Lund, Sweden

A multifunctional NEMS platform based on a mass-producible, surface relief grating has been developed and fabricated directly in polymer materials. The pattern consists of high aspect ratio interdigitated nanometer-sized pairs of walls and can be produced in a low-complexity one-step patterning process with nanoimprint lithography. In this paper, we demonstrate the usefulness of the platform primarily by showing an application as a high-sensitivity mass sensor in air. The sensors, which are based on the high frequency resonant response of around 200 MHz, show a mass responsivity of the order of 0.1 Hz/zg per wall at room temperature and in ambient air. Their ability to selectively adsorb airborne target molecules, such as thiols, is also demonstrated. We also show that the same device can function as a varactor for electronic circuits based on its large tunable capacitive range.



A SEM image of a surface relief grating forming a multifunctional NEMS platform.

Gas sensing properties of single conducting polymer nanowires and the effect of temperature

Yaping Dan¹, Yanyan Cao², Tom E Mallouk², Stephane Evoy³ and AT Charlie Johnson^{1,4}

¹ Department of Electrical Engineering, University of Pennsylvania, Philadelphia, PA 19104, USA

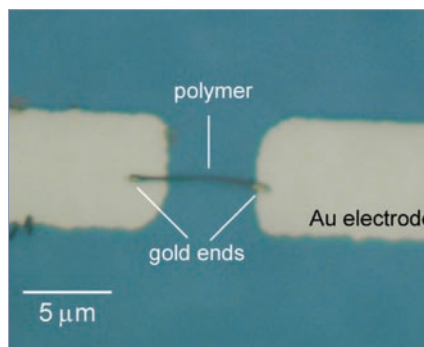
² Department of Chemistry, Pennsylvania State University, College Park, PA 16802, USA

³ Electrical and Computer Engineering and National Institute of Nanotechnology, University of Alberta, Edmonton, AB, T6G 2V4, Canada

⁴ Department of Physics and Astronomy, University of Pennsylvania, Philadelphia, PA 19104, USA

We measured the electronic properties and gas sensing responses of template-grown poly(3,4-ethylenedioxythiophene)/poly(styrenesulfonate) (PEDOT/PSS)-based nanowires. The nanowires had a 'striped' structure

(gold-PEDOT/PSS-gold), and were typically 8 μm long (1 μm –6 μm –1 μm for the sections, respectively) and 220 nm in diameter. Single-nanowire devices were contacted with pre-fabricated gold electrodes using dielectrophoretic assembly. A polymer conductivity of $11.5 \pm 0.7 \text{ S cm}^{-1}$ and a contact resistance of $27.6 \pm 4 \text{ k}\Omega$ were inferred from measurements on nanowires of varying length and diameter. The nanowire sensors detected a variety of odors, with rapid response and recovery (seconds). The response ($\Delta R/R$) varied as a power law with analyte concentration. The power law exponent was found to increase with the molecular weight of the analyte and as a function of temperature. The detection limits are set by noise intrinsic to the device and are at the ppm level even for very volatile analytes.



Optical microscopic image of a striped nanowire assembled onto a pair of gold electrodes.

MATERIALS: PROPERTIES, CHARACTERIZATION OR TOOLS

Effective elastic mechanical properties of single layer graphene sheets

Featured on
nanotechweb.org

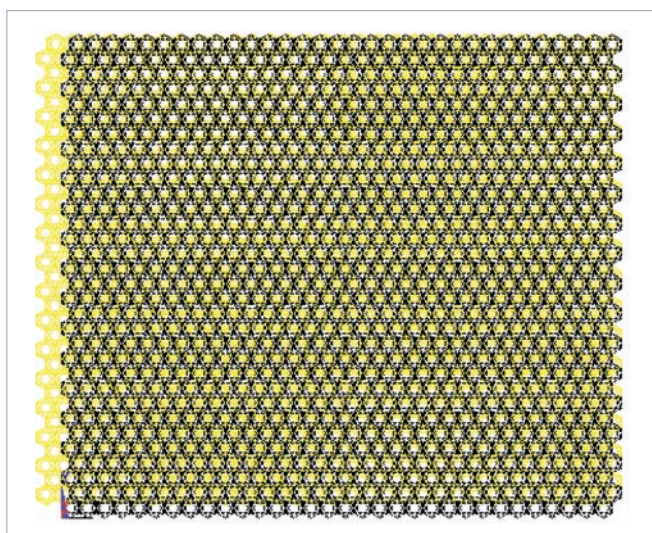
F Scarpa¹, S Adhikari² and A Srikantha Phani³

¹ Department of Aerospace Engineering, University of Bristol, Bristol BS8 1TR, UK

² School of Engineering, University of Wales Swansea, UK

³ Department of Mechanical Engineering, The University of British Columbia, Vancouver, Canada

The elastic moduli of single layer graphene sheet (SLGS) have been a subject of intensive research in recent years. Calculations of these effective properties range from molecular dynamic simulations to use of structural mechanical models. On the basis of mathematical models and calculation methods, several different results have been obtained and these are available in the literature. Existing mechanical models employ Euler–Bernoulli beams rigidly jointed to the lattice atoms. In this paper we propose truss-type analytical models and an approach based on cellular material mechanics theory to describe the in-plane linear elastic properties of the single layer graphene sheets. In the cellular material model, the C–C bonds are represented by equivalent mechanical beams having full stretching, hinging, bending and deep shear beam deformation mechanisms. Closed form expressions for Young's modulus, the shear modulus and Poisson's ratio for the graphene sheets are derived in terms of the equivalent mechanical C–C bond properties. The models presented provide not only quantitative information about the mechanical properties of SLGS, but also insight into the equivalent mechanical deformation mechanisms when the SLGS undergoes small strain uniaxial and pure shear loading. The analytical and numerical results from finite element simulations show good agreement with existing numerical values in the open literature. A peculiar marked auxetic behaviour for the C–C bonds is identified for single graphene sheets under pure shear loading.



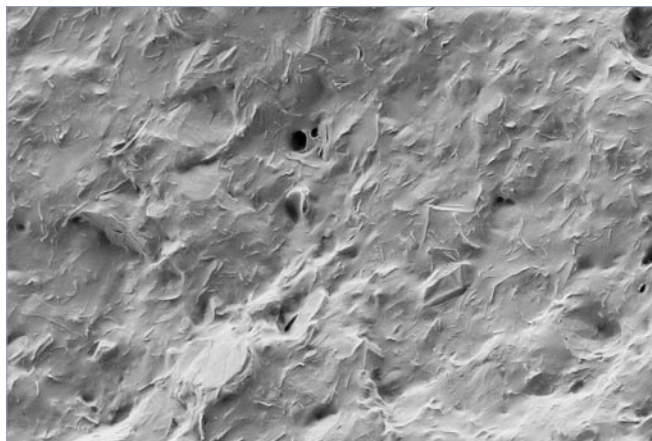
Finite element of braced-truss single layer graphene sheet under tensile stress loading along x-direction.

The mechanical properties and morphology of a graphite oxide nanoplatelet/polyurethane composite

Dongyu Cai, Kamal Yusoh and Mo Song

Department of Materials, Loughborough University, Loughborough, Leicestershire LE11 3TU, UK

Significant reinforcement of polyurethane (PU) using graphite oxide nanoplatelets (GONPs) is reported. Morphologic study shows that, due to the formation of chemical bonding, there is a strong interaction between the GONPs and the hard segment of the PU, which allows effective load transfer. The GONPs can prevent the formation of crystalline hard segments due to their two-dimensional structure. With the incorporation of 4.4 wt% of GONPs, the Young's modulus and hardness of the PU are significantly increased by ~900% and ~327%, respectively. The resultant high resistance to scratching indicates promise for application of these composite materials in surface coating.



SEM image of a 4.4 wt % GONP/PU composite.

Fabrication and characterization of a carbon nanotube-based nanoknife

Featured on
nanotechweb.org

G Singh^{1,2}, P Rice¹, R L Mahajan^{2,3,4} and J R McIntosh⁵

¹ Department of Mechanical Engineering, University of Colorado at Boulder, CO 80309, USA

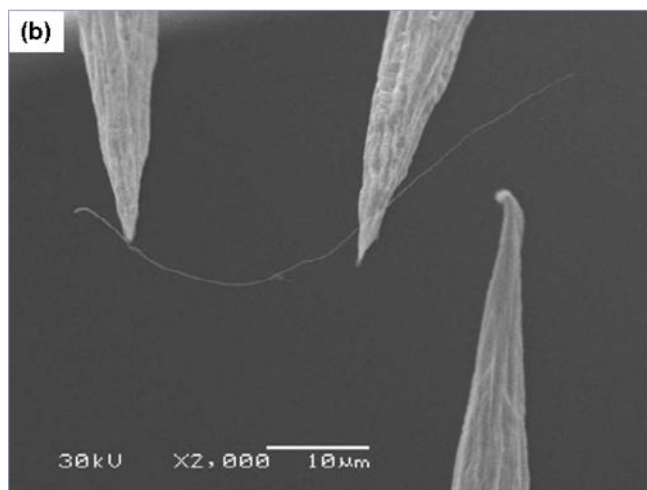
² Institute for Critical Technology and Applied Science, Virginia Polytechnic Institute and State University, Blacksburg, VA 24061, USA

³ Department of Mechanical Engineering, Virginia Polytechnic Institute and State University, Blacksburg, VA 24061, USA

⁴ Department of Engineering Science Mechanics, Virginia Polytechnic Institute and State University, Blacksburg, VA 24061, USA

⁵ Department of Molecular, Cellular and Developmental Biology, University of Colorado at Boulder, CO 80309, USA

We demonstrate the fabrication and testing of a prototype microtome knife based on a multiwalled carbon nanotube (MWCNT) for cutting ~100 nm thick slices of frozen-hydrated biological samples. A piezoelectric-based 3D manipulator was used inside a scanning electron microscope (SEM) to select and position individual MWCNTs, which were subsequently welded in place using electron beam-induced deposition. The knife is built on a pair of tungsten needles with provision to adjust the distance between the needle tips, accommodating various lengths of MWCNTs. We performed experiments to test the mechanical strength of a MWCNT in the completed device using an atomic force microscope tip. An increasing force was applied at the mid-point of the nanotube until failure occurred, which was observed *in situ* in the SEM. The maximum breaking force was approximately (8×10^{-7}) N which corresponds well with the typical microtome cutting forces reported in the literature. *In situ* cutting experiments were performed on a cell biological embedding plastic (epoxy) by pushing it against the nanotube. Initial experiments show indentation marks on the epoxy surface. Quantitative analysis is currently limited by the surface asperities, which have the same dimensions as the nanotube.



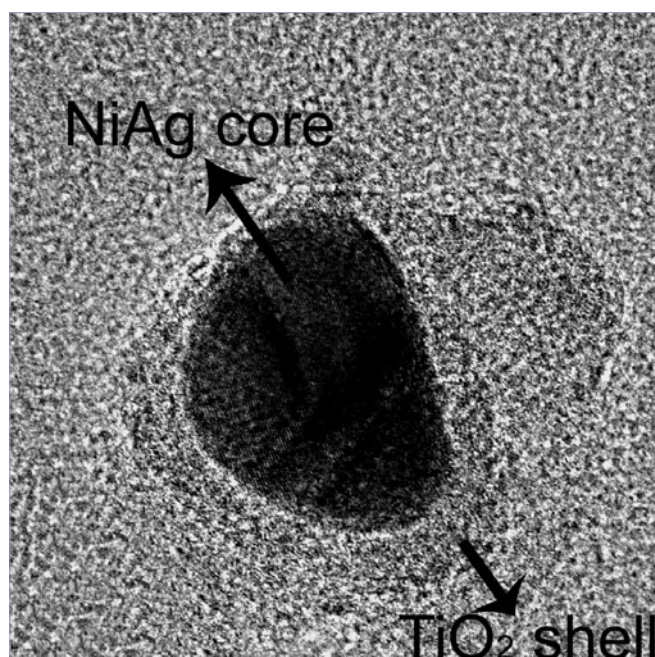
SEM micrograph showing a nanotube welded to a tungsten probe.

Fabrication and photocatalytic activities in visible and UV light regions of Ag@TiO₂ and NiAg@TiO₂ nanoparticles

Haw-Yeu Chuang and Dong-Hwang Chen

Department of Chemical Engineering, National Cheng Kung University, 1, Ta-Hsueh Road, Tainan 701, Taiwan and Center for Micro/Nano Science and Technology, National Cheng Kung University, 1, Ta-Hsueh Road, Tainan 701, Taiwan

Completely discrete Ag@TiO₂ and NiAg@TiO₂ nanoparticles were prepared by the hydrazine reduction of Ag⁺/Ni²⁺ ions and the subsequent sol-gel coating of TiO₂ in an aqueous solution of CTAB. TEM analysis revealed that their core diameters were 6.55 ± 1.20 and 7.57 ± 1.33 nm, respectively, and their shell thicknesses were 2.59 and 2.80 nm, respectively. By the analyses of EDX, UV-vis absorption spectra, FTIR spectra, and zeta potential, their core-shell structure, crystal structure, optical properties, and surface state were demonstrated. In addition to exhibiting significant absorption in the visible light region, it was noted that they had lower zeta potentials than TiO₂ nanoparticles, which favored the adsorption of positively charged organic compounds on the particle surface and thereby increased the photocatalytic reaction rate. By measuring the photocatalytic degradation rate of rhodamine B, Ag@TiO₂ and NiAg@TiO₂ nanoparticles were demonstrated to possess significantly higher photocatalytic activities than TiO₂ nanoparticles in the visible light region because of the formation of Schottky barrier banding at the core-shell interface as well as the excitation of photogenerated electrons from the surface of Ag or NiAg cores to the conduction band of TiO₂ shells. Although NiAg@TiO₂ nanoparticles had lower photocatalytic activity than Ag@TiO₂ nanoparticles owing to weaker surface plasmon resonance, they could be recovered magnetically from the treated solutions. Under UV light illumination, the photocatalytic activities of Ag@TiO₂ and NiAg@TiO₂ nanoparticles were lower than that of TiO₂ nanoparticles because of the lower TiO₂ content and the transfer of photogenerated electrons from TiO₂ shells to Ag or NiAg cores, which also acted as the new recombination centers of photoinduced electrons and holes and hence led to a decrease in the photocatalytic activity.



HRTEM image of NiAg@TiO₂ nanoparticles.

Nano-indentation studies on polymer matrix composites reinforced by few-layer grapheme

Featured on
nanotechweb.org

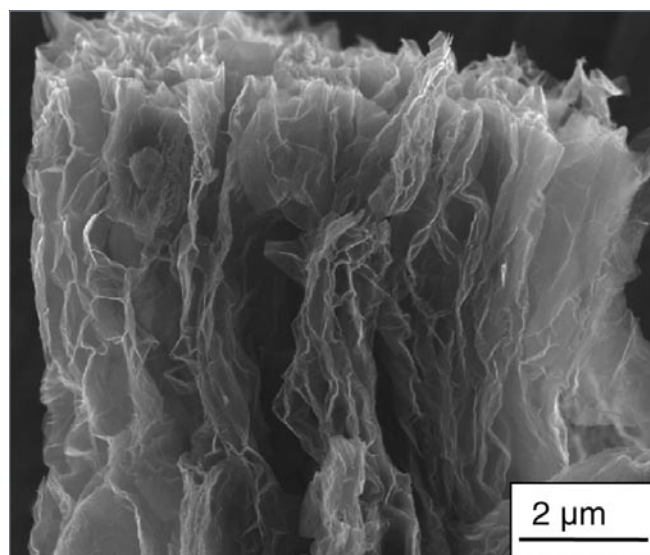
Barun Das^{1,2}, K Eswar Prasad³, U Ramamurty³ and C N R Rao^{1,2}

¹ Chemistry and Physics of Materials Unit and CSIR Centre of Excellence in Chemistry, Jawaharlal Nehru Centre for Advanced Scientific Research, Jakkur PO, Bangalore-560064, India

² Solid State and Structural Chemistry Unit, Indian Institute of Science, Bangalore-560012, India

³ Department of Materials Engineering, Indian Institute of Science, Bangalore-560012, India

The mechanical properties of polyvinyl alcohol (PVA) and poly(methyl methacrylate) (PMMA)-matrix composites reinforced by functionalized few-layer graphene (FG) have been evaluated using the nano-indentation technique. A significant increase in both the elastic modulus and hardness is observed with the addition of 0.6 wt% of graphene. The crystallinity of PVA also increases with the addition of FG. This and the good mechanical interaction between the polymer and the FG, which provides better load transfer between the matrix and the fiber, are suggested to be responsible for the observed improvement in mechanical properties of the polymers.



FESEM image of as prepared exfoliated graphene showing the wrinkled nature of graphene.

Did you know?
Nanotechnology's impact factor
3.446*

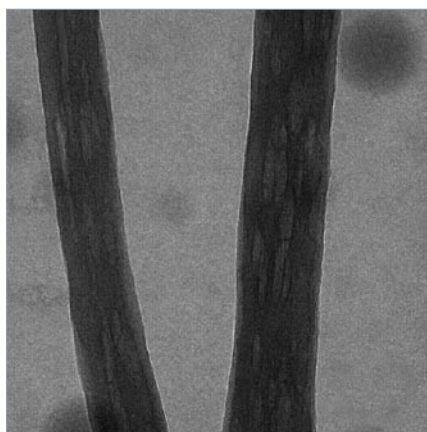
* As listed by the ISI 2008 Science Citation Index Journals Citation Reports

Fabrication of porous carbon nanofibers and their application as anode materials for rechargeable lithium-ion batteries

Liwen Ji and Xiangwu Zhang

Fiber and Polymer Science Program, Department of Textile Engineering, Chemistry and Science, North Carolina State University, Raleigh, NC 27695-8301, USA

Porous carbon nanofibers were prepared by the electrospinning of a bicomponent polymer solution, followed by thermal treatments under different atmospheres. The surface morphology, thermal properties, and crystalline features of these nanofibers were characterized using various analytic techniques, and it was found that they were formed with turbostratically disordered graphene sheets and had small pores and large surface areas. The unique structure of these porous carbon nanofibers resulted in good electrochemical performance such as high reversible capacity and good cycle stability when they were used as anodes for rechargeable lithium-ion batteries.



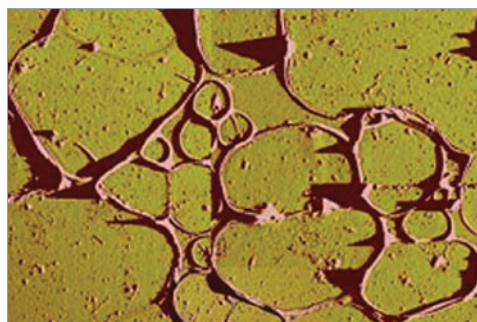
TEM image of porous carbon nanofibers made from PAN/PLLA (9:1) nanofibres.

A new AFM–HRTEM combined technique for probing isolated carbon nanotubes

Shota Kuwahara, Toshiki Sugai and Hisanori Shinohara

Department of Chemistry and Institute for Advanced Research, Nagoya University, Nagoya 464-8602, Japan

A new technique has been developed for characterizing individual carbon nanotubes (CNTs). This technique combines atomic force microscopy (AFM) measurements with an independent determination of the CNT structure obtained by using thin carbon grid membranes for high-resolution transmission electron microscopy (HRTEM) measurements. The membrane grids are easily transferred onto silicon oxide substrates, where they are observed by AFM and an optical charged-coupled device. Electrostatic force microscopy measurements are also performed on single- and double-walled CNTs whose structures had previously been determined by HRTEM. The results reveal that the diameter and outer tube length have a greater effect on determining the capacitance of the nanotubes than the presence of the inner tube of double-walled CNTs.



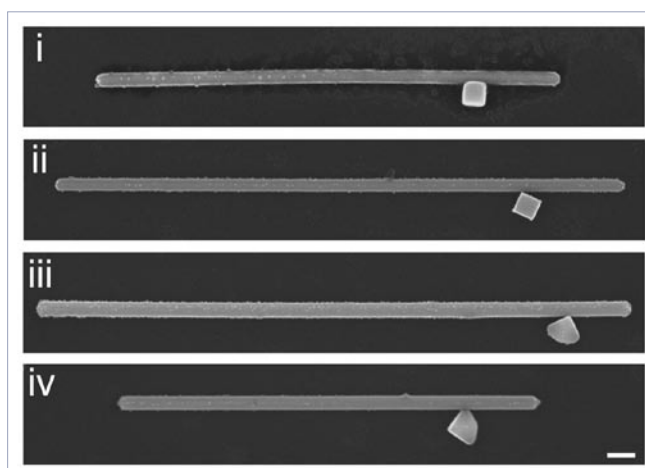
AFM image showing a carbon grid membrane. The image was taken following transfer printing of the membrane onto a silicon oxide substrate.

Measuring the surface-enhanced Raman scattering enhancement factors of hot spots formed between an individual Ag nanowire and a single Ag nanocube

Pedro H C Camargo, Claire M Cobley, Matthew Rycenga and Younan Xia

Department of Biomedical Engineering, Washington University, St Louis, MO 63130, USA

This paper describes a systematic study of the surface-enhanced Raman scattering (SERS) activity of hot spots formed between a Ag nanowire and a Ag nanocube with sharp corners. We investigated two distinct dimer structures: (i) a nanocube having one side face nearly touching the side face of a nanowire, and (ii) a nanocube having one edge nearly touching the side face of a nanowire. The field enhancements for the dimers displayed a strong dependence on laser polarization, and the strongest SERS intensities were observed for polarization along the hot-spot axis. Moreover, the detected SERS intensities were dependent on the hot-spot structure, i.e., the relative orientation of the Ag nanocube with respect to the nanowire's side face. When the dimer had a face-to-face configuration, the enhancement factor E_{dimer} was 1.4×10^7 . This corresponds to 22-fold and 24-fold increases compared to those for individual Ag nanowires and nanocubes, respectively. Conversely, when the dimer had an edge-to-face configuration, E_{dimer} was 4.3×10^6 . These results demonstrated that the number of probe molecules adsorbed at the hot spot played an important role in determining the detected SERS intensities. E_{dimer} was maximized when the dimer configuration allowed for a larger number of probe molecules to be trapped within the hot-spot region.



SEM image showing 4 nanowires, each with a nanocube attached at a different orientation.

EDITORIAL BOARD

Editor-in-Chief

Mark Reed, Yale University, CT, USA

Section Editors

Biology and medicine

Andreas Engel, Universität Basel, Switzerland

Electronics and photonics

Meyya Meyyappan, NASA Ames Research Center, CA, USA

Patterning and nanofabrication

Alfred Forchel, Julius Maximilians University, Würzburg, Germany

Quantum phenomena

Daniel Loss, Universität Basel, Switzerland

Sensing and actuating

Juergen Brugger, Ecole Polytechnique Federale de Lausanne, Switzerland

Materials: synthesis and self-assembly

Tom Mallouk, Pennsylvania State University, PA, USA

Materials: properties, characterization and tools

Mervyn Miles, University of Bristol, UK

Editorial Board

David Awschalom, University of California, Santa Barbara, CA, USA

Chunli Bai, Chinese Academy of Sciences, China

Yoshio Bando, National Institute for Materials Science, Japan

Christian Brosseau, Université de Bretagne Occidentale, France

Harold Craighead, Cornell University, NY, USA

Christoph Gerber, Universität Basel, Switzerland

George Gruner, Unidym, CA, USA

Peter Grutter, McGill University, Canada

Devens Gust, Arizona State University, AZ, USA

Dae Joon Kang, Sungkyunkwan University, Korea

Jeffrey Karp, Massachusetts Institute of Technology, MA, USA

Michael Roukes, California Institute of Technology, CA, USA

Mark Saltzmann, Yale University, CT, USA

John Shelnett, Sandia National Laboratories, NM, USA

Mark Spearing, University of Southampton, UK

Samuel Stupp, Northwestern University, IL, USA

Jonas Tegenfeldt, Lund University, Sweden

Zhong-Lin Wang, Georgia Institute of Technology, GA, USA

Mark Welland, University of Cambridge, UK

George Whitesides, Harvard University, MA, USA

Roland Wiesendanger, Universität Hamburg, Germany

JOURNAL TEAM



Anna Demming
Publishing Editor



Natalie Green
Publishing Administrator



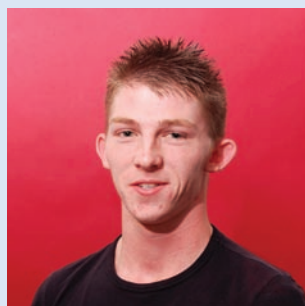
Amy Harvey
Publishing Editor



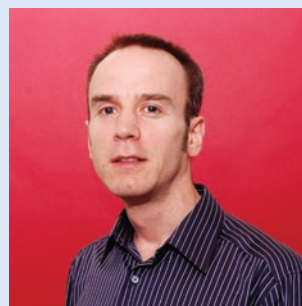
Rachel Lawless
Publishing Editor



Holly Purcell
Marketing Executive



Danny Turner
Publishing Administrator



James Tyrrell
Editor, nanotechweb.org



Alex Wotherspoon
Publisher



A downloadable case study that provides an overview of your product.

Tell our readers about your products

White papers provide the opportunity to obtain qualified sales leads as the readers' details are captured with each free download and sent to the advertiser.

To start generating sales leads today, call David Iddon on +44 (0)117 930 1032
or e-mail david.iddon@iop.org

WHY PUBLISH WITH NANOTECHNOLOGY?

1. HIGH IMPACT

The growth in the number of published articles has been accompanied by an impressive increase in the impact factor. *Nanotechnology* has an impact factor of 3.446 as listed by the ISI 2008 Science Citation Index Journal Citation Report.

2. FAST PUBLICATION

Our peer review process is rigorous and efficient, with a receipt to first decision time of just 21 days.

3. INTERNATIONAL READERSHIP

Over 100 countries worldwide have access to all articles published in *Nanotechnology*, making the journal truly international.

AND THAT'S NOT ALL...

By publishing your paper with *Nanotechnology* you can take advantage of a number of other benefits including:

- **Free for 30 days**

All articles published in *Nanotechnology* are free to read for all, for the first 30 days following publication.

- **Nanotechweb.org**

Additional promotional opportunities are available on our sister website **nanotechweb.org**, which is viewed by more than 53,000 people per month.

- **Work with the best**

Nanotechnology features top research from institutions throughout the world; only 27% of submitted articles are accepted for publication.

- **Widely read**

Over 1 million *Nanotechnology* articles were downloaded through 2008.

- **Fantastic visibility and exposure**

The journal will be represented at over 30 conferences in 2010.

DO YOU WANT TO KNOW MORE?

To find out more about publishing with *Nanotechnology*, please visit **www.iop.org/EJ/nano** or contact the journal team at **nano@iop.org**



nanobio

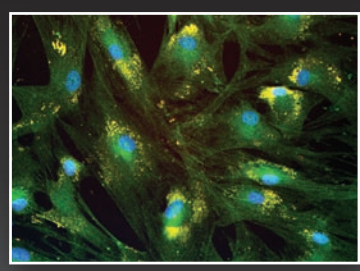
patterning on the desktop



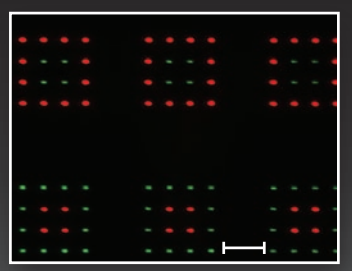
NLP 2000 System

desktop nanofabrication platform

- multiplexing capabilities
- infinite molecule – substrate combinations
- sub-micron / nanoscale feature sizes
- no cleanroom needed



Stem cell adhesion and spreading on a patterned substrate.



Multiplexing of PEG dot arrays deposited onto a glass slide. Scale bar = 20 μ m.

please visit Nanolnk at: www.nanoink.net
or call us at: 1-847-679-NANO

IOP Publishing
Dirac House, Temple Back, Bristol BS1 6BE UK
Tel: +44 (0)117 929 7481 Fax: +44 (0)117 929 4318
Email: nano@iop.org Website: www.iop.org/EJ/nano